Acta Cryst E CRYSTALLOGRAPHIC COMMUNICATIONS

ISSN 2056-9890

Bis(*N*,*N*-diethyldithiocarbamato-$\kappa^2 S,S'$)(3-hydroxypyridine-κN)zinc and bis[*N*-(2-hydroxyethyl)-*N*-methyldithiocarbamato-$\kappa^2 S,S'$](3-hydroxypyridine-κN)zinc: crystal structures and Hirshfeld surface analysis

Received 25 October 2016
Accepted 27 October 2016

Edited by W. T. A. Harrison, University of Aberdeen, Scotland

‡ Additional correspondence author, e-mail: mmjotani@rediffmail.com.

Keywords: crystal structure; zinc; dithiocarbamate; hydroxypyridine; hydrogen bonding; Hirshfeld surface analysis.

CCDC references: 1511865; 1511864

Supporting information: this article has supporting information at journals.iucr.org/e

Mukesh M. Jotani,[a]‡ Hadi D. Arman,[b] Pavel Poplaukhin[c] and Edward R. T. Tiekink[d]*

[a]Department of Physics, Bhavan's Sheth R. A. College of Science, Ahmedabad, Gujarat 380 001, India, [b]Department of Chemistry, The University of Texas at San Antonio, One UTSA Circle, San Antonio, Texas 78249-0698, USA, [c]Chemical Abstracts Service, 2540 Olentangy River Rd, Columbus, Ohio, 43202, USA, and [d]Research Centre for Crystalline Materials, Faculty of Science and Technology, Sunway University, 47500 Bandar Sunway, Selangor Darul Ehsan, Malaysia. *Correspondence e-mail: edwardt@sunway.edu.my

The common feature of the molecular structures of the title compounds, $[Zn(C_5H_{10}NS_2)_2(C_5H_5NO)]$, (I), and $[Zn(C_4H_8NOS_2)_2(C_5H_5NO)]$, (II), are NS_4 donor sets derived from *N*-bound hydroxypyridyl ligands and asymmetrically chelating dithiocarbamate ligands. The resulting coordination geometries are highly distorted, being intermediate between square pyramidal and trigonal bipyramidal for both independent molecules comprising the asymmetric unit of (I), and significantly closer towards square pyramidal in (II). The key feature of the molecular packing in (I) is the formation of centrosymmetric, dimeric aggregates sustained by pairs of hydroxy-O—H···S(dithiocarbamate) hydrogen bonds. The aggregates are connected into a three-dimensional architecture by methylene-C—H···O(hydroxy) and methyl-C—H···π(chelate) interactions. With greater hydrogen-bonding potential, supramolecular chains along the *c* axis are formed in the crystal of (II), sustained by hydroxy-O—H···O(hydroxy) hydrogen bonds, with ethylhydroxy and pyridylhydroxy groups as the donors, along with ethylhydroxy-O—H···S(dithiocarbamate) hydrogen bonds. Chains are connected into layers in the *ac* plane by methylene-C—H···π(chelate) interactions and these stack along the *b* axis, with no directional interactions between them. An analysis of the Hirshfeld surfaces clearly distinguished the independent molecules of (I) and reveals the importance of the C—H···π(chelate) interactions in the packing of both (I) and (II).

1. Chemical context

The structures of binary zinc bis(dithiocarbamates) are always zero-dimensional (*i.e.* molecular) (Heard, 2005) in contrast to their cadmium (Tan *et al.*, 2016*b*) and mercury (Jotani *et al.*, 2016) analogues; dithiocarbamate is $^-S_2CNRR'$. The zinc structures can be mononuclear, distorted tetrahedral as in $Zn(S_2CNCy_2)_2$ (Cox & Tiekink, 2009) or, far more commonly, binuclear as in the archetypical compound $[Zn(S_2CNEt_2)_2]_2$, where heavily distorted five-coordinate geometries are found for zinc as two of the ligands are chelating and the others are μ_2-tridentate (Bonamico *et al.*, 1965; Tiekink, 2000), with the adoption of one form over the other often being related to the steric bulk of the *R*/*R*′ groups (Tiekink, 2003). However, there is no clear-cut delineation between the adoption of one structural motif over the other depending on steric bulk. This is nicely illustrated in the structure of $Zn[S_2CN(i\text{-}Bu)_2]_2$ which

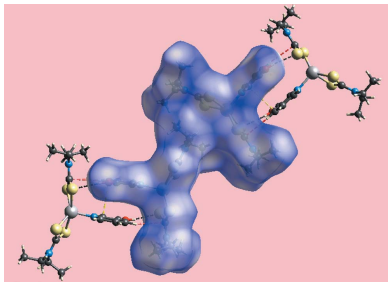

has equal numbers of both motifs (Ivanov *et al.*, 2005). A popular process by which structures of greater dimensionality might be formed is by the addition of neutral, potentially bridging ligands. However, in the case of zinc dithiocarbamates, complexation with bidentate ligands usually results in the isolation of zero-dimensional, binuclear molecules, *e.g.* $\{Zn[S_2CN(Me)i\text{-}Pr)]_2\}_2(Me_2NCH_2CH_2NMe_2)$ (Malik *et al.*, 1997); $[Zn(S_2CNMe_2)_2]_2$(4,4′-bipyridyl) (Zha *et al.*, 2010) and $[Zn(S_2CNEt_2)_2]_2(Ph_2PCH_2CH_2PPh_2)$ (Zeng *et al.*, 1994). Even when excess base is included in the reaction, *e.g. trans*-1,2-bis(4-pyridyl)ethylene (bpe), only the zero-dimensional binuclear compound is isolated with non-coordinating bpe solvate, *i.e.* $Zn(S_2CNEt_2)_2]_2$(bpe)·bpe (Lai & Tiekink, 2003). That this reluctance to form coordination polymers is related directly to the nature of the dithiocarbamate ligand is seen in the adoption of zigzag chains in analogous xanthate complexes, *e.g.* $\{[Zn(S_2COR)_2]_2(bpe)\}_n$, for R = Et and *n*-Bu (Kang *et al.*, 2010). Steric effects come into play when R = Cy whereby a binuclear species is isolated, *i.e.* $[Zn(S_2COCy)_2]_2$(bpe) (Kang *et al.*, 2010). This difference in chemistry arises to the significant (40%) contribution of the canonical structure $^{(2-)}S_2CN^{(+)}RR'$, with two formally negatively charged sulfur atoms, which makes dithiocarbamate a very effective chelating agent, thereby decreasing the Lewis acidity of the zinc atom.

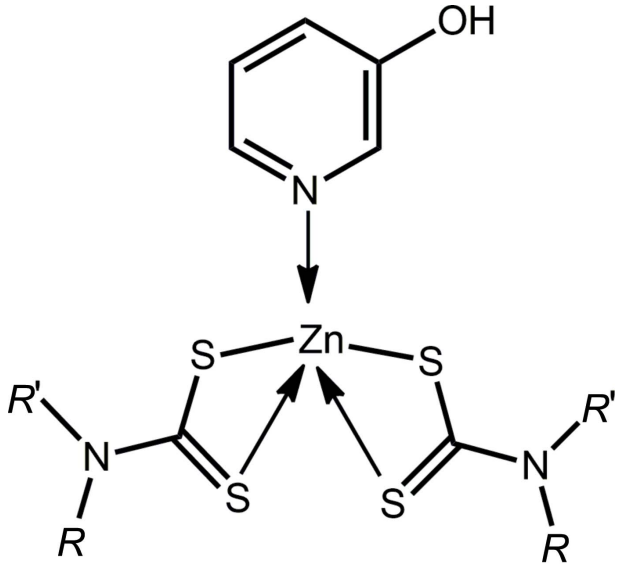

(I) $R = R' =$ Et

(II) $R =$ Me, $R' = CH_2CH_2OH$

An approach to increase the supramolecular aggregation in the crystal structures of zinc dithiocarbamates has been to introduce hydrogen bonding functionality into the ligands, *i.e* using dithiocarbamate anions of the type $^{-}S_2CN(R)CH_2CH_2OH$. This influence is seen in the recent report of the structures of $Zn[S_2CN(R)CH_2CH_2OH]_2$(2,2′-bipyridyl) for R = *i*-Pr and CH_2CH_2OH (Safbri *et al.*, 2016). The common feature of these structures along with those of related species with no hydrogen bonding potential, *e.g.*

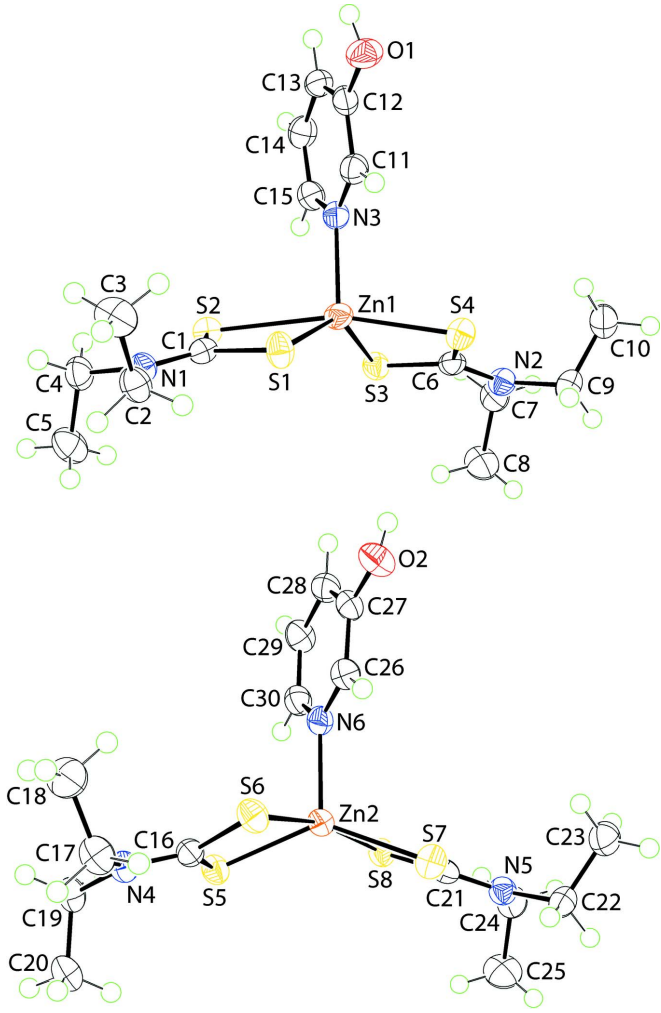

Figure 1
The molecular structures of the two independent molecules comprising the asymmetric unit in (I), showing the atom-labelling scheme and displacement ellipsoids at the 70% probability level.

$Zn(S_2CNMe_2)_2$(2,2′-bipyridyl) (Manohar *et al.*, 1998), is the presence of a distorted octahedral N_2S_4 donor set about the zinc atom. The O—H···O hydrogen bonding in $Zn[S_2CN(R)CH_2CH_2OH]_2$(2,2′-bipyridyl), in the case when R = CH_2CH_2OH, isolated as a 1:1 hydrate, leads to supramolecular ladders and these extend in two dimensions *via* water-O—H···S(dithiocarbamate) hydrogen bonds. When R = *i*-Pr, layers are sustained by hydroxy-O—H···S hydrogen bonds (Safbri *et al.*, 2016). As an extension of these studies, in the present report, $Zn(S_2CNRR')_2$ has been complexed with 3-hydroxypyridine (pyOH) to yield two 1:1 complexes. Quite different aggregation patterns are observed when $R = R'$ = Et (I), and R = *i*-Pr and R' = CH_2CH_2OH (II). The crystal and molecular structures of (I) and (II) are described herein along with an analysis of their Hirshfeld surfaces.

2. Structural commentary

Two independent molecules of $Zn(S_2CNEt_2)_2$(pyOH) comprise the asymmetric unit of (I), Fig. 1; pyOH is

Table 1
Geometric data (Å, °) for (I) and (II).

Parameter	Zn1-molecule in (I)	Zn2-molecule in (I)	(II)
Zn—S1	2.3201 (8)	–	2.3319 (6)
Zn—S2	2.7461 (8)	–	2.7514 (8)
Zn—S3	2.3417 (8)	–	2.3437 (7)
Zn—S4	2.4932 (8)	–	2.5275 (6)
Zn—S5	–	2.3399 (8)	–
Zn—S6	–	2.5453 (8)	–
Zn—S7	–	2.3517 (8)	–
Zn—S8	–	2.6051 (8)	–
Zn—N3	2.069 (2)	–	2.0375 (16)
Zn—N6	–	2.070 (2)	–
C—S1, S2	1.736 (3), 1.721 (3)	–	1.733 (2), 1.7119 (19)
C—S3, S4	1.741 (3), 1.720 (3)	–	1.7364 (19), 1.7140 (19)
C—S5, S6	–	1.743 (3), 1.720 (3)	–
C—S7, S8	–	1.734 (3), 1.730 (3)	–
S1—Zn—S2	70.99 (3)	–	70.825 (18)
S3—Zn—S4	75.54 (3)	–	74.41 (2)
S1—Zn—S3	136.44 (3)	–	139.04 (2)
S2—Zn—S4	165.17 (2)	–	148.839 (18)
S5—Zn—S6	–	74.34 (3)	–
S7—Zn—S8	–	73.08 (3)	–
S5—Zn—S7	–	137.08 (3)	–
S6—Zn—S8	–	168.91 (2)	–
S1,S2,C1/S3,S4,*C*	19.30 (12)	–	63.81 (15)
S5,S6,C1/S7,S8,*C*	–	38.87 (22)	–

3-hydroxypyridine. For the Zn1-containing molecule, Fig. 1*a*, the Zn^{II} atom is chelated by two dithiocarbamate ligands and one nitrogen atom derived from the monodentate pyOH ligand. The S1-dithiocarbamate ligand chelates the zinc atom forming quite different Zn—S bond lengths compared with the S3-dithiocarbamate ligand. This is quantified in the values of Δ(Zn—S), being the difference between the $Zn—S_{long}$ and $Zn—S_{short}$ bond lengths, Table 1, *i.e.* 0.43 and 0.15 Å, respectively. The Zn1—N3 bond length is significantly shorter than the Zn—S bonds. The NS_4 coordination geometry is highly distorted as seen in the value of τ of 0.48 (Addison *et al.*, 1984).

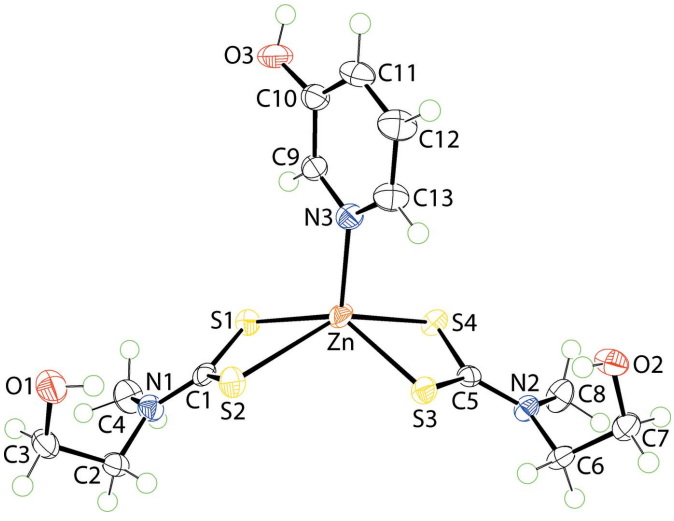

Figure 2
The molecular structure of (II), showing the atom-labelling scheme and displacement ellipsoids at the 70% probability level.

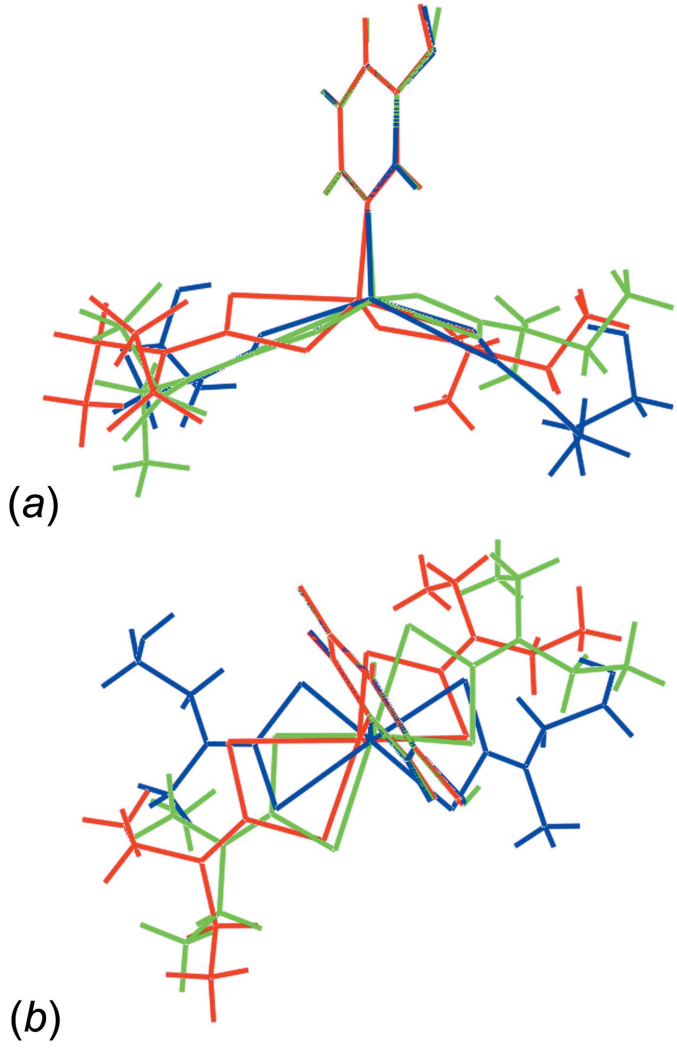

Figure 3
Overlay diagrams for the Zn1- and Zn2-molecules in (I) and the molecule in (II) shown as red, green and blue images, respectively: (*a*) approximately side-on to the pyOH ring and (*b*) along the N—Zn bond. The molecules are overlapped so that the pyOH rings are coincident.

This value is almost exactly intermediate between the ideal square pyramidal geometry with τ = 0.0 and ideal trigonal pyramidal with τ = 1.0. The acute S—Zn—S chelate angles contribute to this distortion, Table 1. The widest angles in the coordination geometry are subtended by $S_s—Zn—S_s$ (s = short) and, especially, the $S_l—Zn—S_l$ (l = long) bond angles, Table 1. The coordination geometry for the Zn2 atom, Fig. 1*b*, is quite similar to that just described for the Zn1 atom. The values of Δ(Zn—S) of 0.21 and 0.25 Å are intermediate to those for the Zn1-molecule. Even so, the differences in the Zn—S bond lengths in both molecules are not that great with this observation reflected in the closeness of the C—S bond lengths, Table 1. The value of τ for the Zn2-molecule is 0.53, indicating an inclination towards trigonal bipyramidal *cf.* the Zn1-molecule.

The molecular structure of (II), $Zn[S_2CN(Me)CH_2CH_2OH]_2(pyOH)$, is shown in Fig. 2 and selected geometric parameters are included in Table 1. The coordination modes

Table 2
Hydrogen-bond geometry (Å, °) for (I).

*Cg*1 and *Cg*2 are the centroids of the (Zn1,S1,S2,C1) and (Zn2,S7,S8,C21) chelate rings, respectively.

D—H···*A*	*D*—H	H···*A*	*D*···*A*	*D*—H···*A*
O1—H1*O*···S8^{i}	0.84 (2)	2.45 (1)	3.289 (2)	173 (4)
O2—H2*O*···S2^{ii}	0.84 (2)	2.31 (1)	3.143 (2)	170 (4)
C8—H8*A*···*Cg*2	0.98	2.98	3.855 (3)	150
C13—H13···*Cg*2^{i}	0.95	2.79	3.631 (3)	148
C20—H20*C*···*Cg*1^{iii}	0.98	2.97	3.850 (3)	150
C28—H28···*Cg*1^{ii}	0.95	2.96	3.738 (3)	140
C19—H19*A*···O2^{iv}	0.99	2.56	3.321 (3)	134

Symmetry codes: (i) $-x+1, y+\frac{1}{2}, -z+\frac{1}{2}$; (ii) $-x+1, y-\frac{1}{2}, -z+\frac{1}{2}$; (iii) $x+1, y, z$; (iv) $x, -y+\frac{1}{2}, z-\frac{1}{2}$.

Table 3
Hydrogen-bond geometry (Å, °) for (II).

*Cg*1 is the centroid of the (Zn,S3,S4,C5) chelate ring.

D—H···*A*	*D*—H	H···*A*	*D*···*A*	*D*—H···*A*
O1—H1*O*···S2	0.84 (2)	2.61 (2)	3.371 (2)	152 (3)
O2—H2*O*···O1^{i}	0.83 (3)	1.94 (3)	2.734 (2)	161 (3)
O3—H3*O*···O2^{ii}	0.84 (3)	1.79 (2)	2.619 (2)	170 (3)
C2—H2*B*···*Cg*1^{iii}	0.99	2.76	3.689 (2)	156

Symmetry codes: (i) $-x+1, -y+1, -z$; (ii) $-x+1, -y+1, -z+1$; (iii) $-x+2, -y+1, -z$.

of the dithiocarbamate ligands in (II) are close to those observed for the Zn1-molecule in (I) with Δ(Zn—S) values of 0.42 and 0.19 Å. The difference between (I) and (II) is found in the coordination geometry which is close to square pyramidal in (II), as seen in the value of τ = 0.16. In this description, the S1–S4 atoms define the basal plane with the r.m.s. deviation being 0.0501 Å. The Zn atom lies 0.7514 (4) Å above the plane in the direction of the N3 atom. The dihedral angle between the chelate rings is 63.81 (15)°, an angle significantly greater than for the comparable angles in (I), Table 1.

Overlay diagrams of the three molecules in (I) and (II) are shown in Fig. 3. The molecules have been overlapped so that the pyOH rings are coincident. The differences in the conformations of the molecules comprising (I) are clearly seen, and especially between these and the conformation in (II). Such variability in structure reflects the flexibility in the binding modes of the dithiocarbamate ligands leading to quite distinctive coordination geometries.

3. Supramolecular features

The key feature of the molecular packing of (I) is the formation of hydroxy-O—H···S(dithiocarbamate) hydrogen bonds that sustain centrosymmetric, dimeric aggregates, *via* a 14-membered $\{\cdots HOC_2NZnS\}_2$ synthon, Fig. 4*a* and Table 2. Additional stabilization to the dimer is provided by an intradimer π–π interaction between the pyOH rings. The intercentroid distance is 3.5484 (18) Å and the angle of inclination is 3.91 (14)° for symmetry operation $1-x, \frac{1}{2}+y, \frac{1}{2}-z$. The aggregates are further stabilized by pyOH-C—H···π interactions where the π-system is a chelate ring. Such C—H···π(chelate) interactions are increasingly being recognized as being important in the supramolecular chemistry of metal 1,1-dithiolates (Tiekink & Zukerman-Schpector, 2011; Tan *et al.*, 2016*a*) and, it should be noted, routinely appear in the output from *PLATON* (Spek, 2009). Connections between aggregates leading to supramolecular layers in the *ab* plane are also of the type C—H···π(chelate) but with methyl-H atoms as the donors, Fig. 4*b*. The connections between layers along the *c* direction are of the type methylene-C—H···O(hydroxy), Fig. 4*c*.

The addition of greater hydrogen-bonding potential in (II) results in an infinite chain, Table 3. There is an hydroxy-O—H···O(hydroxy) hydrogen bond involving the O2 and O1 atoms as the donor and acceptor, respectively. The O1-hydroxy group forms a hydrogen bond with a dithiocarbamate-S2 atom. As shown by the '1' in Fig. 5*a*, these hydrogen bonds lead to a centrosymmetric 22-membered $\{\cdots SZnSCNC_2OH\cdots OH\}_2$ synthon. On either side of these

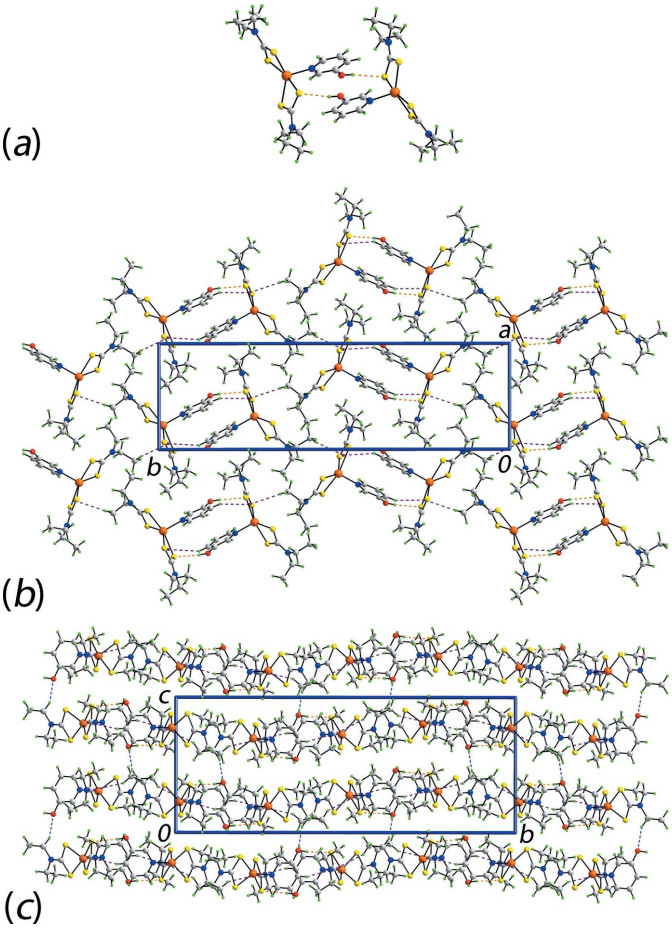

Figure 4
The molecular packing in (I), showing (*a*) detail of the hydroxy-O—H···S(dithiocarbamate) hydrogen bonding, shown as orange dashed lines, leading to dimeric aggregates, (*b*) supramolecular layer where the aggregates in (*a*) are linked by C—H···π(chelate) interactions, shown as purple dashed lines and (*c*) view of the unit-cell contents shown in projection down the *a* axis, with links between layers being of the type C—H···O, shown as blue dashed lines.

synthons, the pyOH hydroxy group hydrogen bonds to the O2-hydroxy atom and through symmetry, a centrosymmetric 24-membered $\{\cdots OC_2NCSZnNC_2OH\}_2$ synthon is formed, highlighted as '2' in Fig. 5*a*. Alternating synthons generate a supramolecular chain aligned along the *c* axis. Methylene-C—H$\cdots\pi$(chelate) interactions link molecules into dimeric units, Fig. 5*b*. The combination of the aforementioned interactions lead to supramolecular layers that stack along the *b* axis with no directional interactions between them, Fig. 5*c*.

4. Hirshfeld surface analysis

The Hirshfeld surface analysis for (I) and (II) was performed as described recently (Cardoso *et al.*, 2016). From the views of the Hirshfeld surface mapped over d_{norm} in the range −0.2 to +1.3 au for the Zn1- and Zn2-containing molecules of (I), Fig. 6, the presence of bright-red spots near the hydroxy-H1*O* and -H2*O*, and dithiocarbamate-S2 and S8 atoms represent the donors and acceptors of the O—H$\cdots$S hydrogen bonds; these are viewed as blue and red regions on the Hirshfeld surfaces mapped over electrostatic potential (mapped over the range −0.07 to +0.10 au), Fig. 7, corresponding to positive and negative potentials, respectively. The faint-red spots appearing near the hydroxy-O2 and methyl-C19 atoms in Fig. 6*b* and 6*c* are due to comparatively weaker intermolecular C—H$\cdots$O interactions. The intra-dimer π–π stacking interaction between the pyOH rings, Fig. 4*a*, is evident through the appearance of faint-red spots near the arene-C13 and C26 atoms of the rings, Fig. 6*a* and 6*b*, forming a close interatomic C$\cdots$C contact, Table 4. The diminutive-red spots near the pyOH-H13 and -H28 and dithiocarbamate-C21 atoms, Fig. 6*a*–*c*, characterize the influence of the C—H$\cdots\pi$(chelate) interactions; in Fig. 7, the light-blue and red regions represent the respective donors and acceptors for these interactions. The

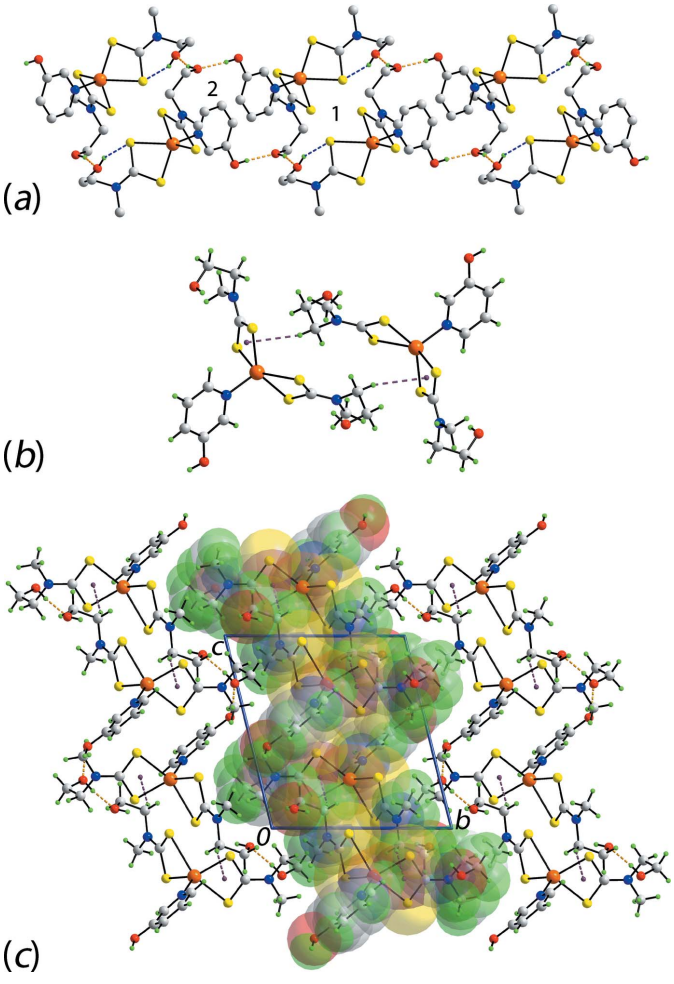

Figure 5
The molecular packing in (II), (*a*) supramolecular chain mediated by hydroxy-O—H$\cdots$O(hydroxyl), S(dithiocarbamate) hydrogen bonding, shown as orange and blue dashed lines, respectively, and non-acidic H atoms omitted, (*b*) detail of methylene-C—H$\cdots\pi$(chelate) interactions shown as purple dashed lines and (*c*) view of the unit-cell contents shown in projection down the *a* axis, with one layer shown in space-filling mode.

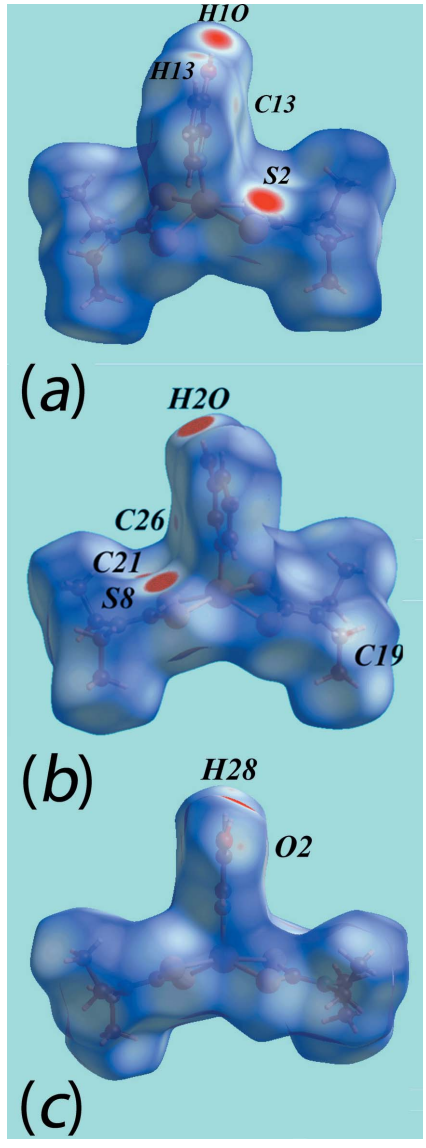

Figure 6
Views of the Hirshfeld surfaces for (I) mapped over d_{norm} for the (*a*) Zn1-molecule and, (*b*) and (*c*) Zn2-molecule.

Table 4
Summary of short interatomic contacts (Å) in (I) and (II).

Contact	Distance	Symmetry operation
(I)		
C13···C26	3.314 (4)	$1-x, \frac{1}{2}+y, \frac{1}{2}-z$
H5···H7*B*	2.36	$-x, 1-y, -z$
O1···H18*B*	2.61	$2-x, 1-y, 1-z$
S2···H20*B*	2.96	$1-x, 1-y, -z$
S4···H11	2.98	$1-x, 1-y, 1-z$
S5···H7*A*	2.97	x, y, z
S5···H14	2.94	$1-x, 1-y, -z$
C1···H28	2.75	$1-x, \frac{1}{2}+y, \frac{1}{2}-z$
C21···H13	2.65	$1-x, -\frac{1}{2}+y, \frac{1}{2}-z$
C29···H24*A*	2.84	$1+x, y, z$
(II)		
S4···S4	3.4765 (11)	$2-x, 1-y, 1-z$
C8···C8	3.308 (3)	$2-x, -y, 1-z$
C1···H6*A*	2.87	$x, 1+y, z$
C9···H7*B*	2.57	$x, 1+y, z$
C10···H10*B*	2.88	$x, 1+y, z$
H1*O*···H2*O*	2.37 (4)	$1-x, 1-y, -z$
H2*O*···H3*O*	2.18 (3)	$1-x, 1-y, 1-z$
S3···H1*O*	2.91 (3)	$1-x, 1-y, -z$
S3···H7*A*	2.99	$1-x, 1-y, -z$
Zn···H2*B*	3.06	$2-x, 1-y, -z$
O1···H6*A*	2.68	$x, 1+y, z$

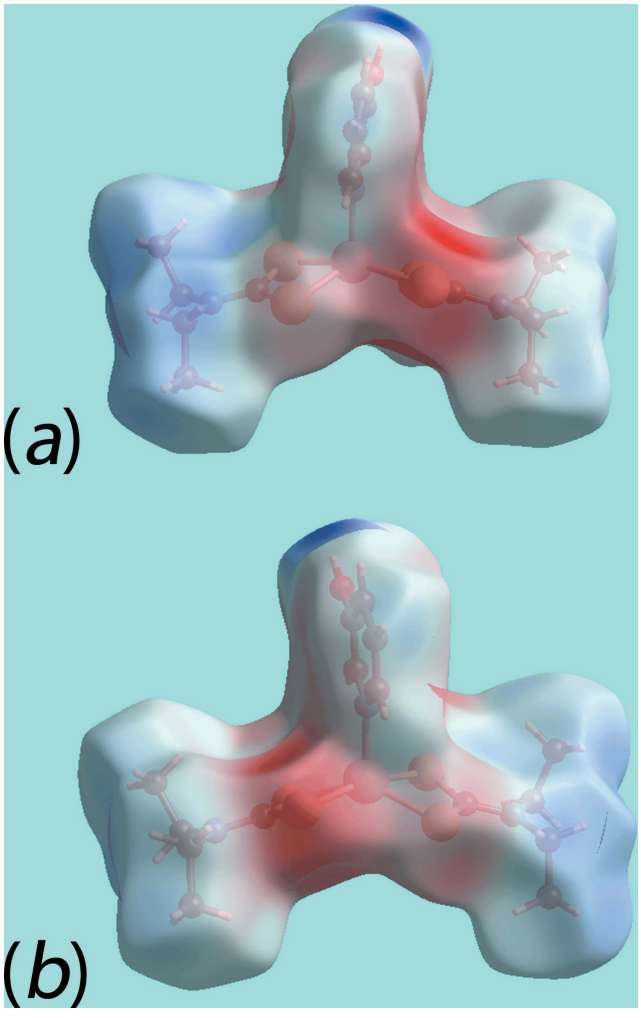

Figure 7
Views of the Hirshfeld surfaces mapped over electrostatic potential for (I): (*a*) Zn1-molecule and (*b*) Zn2-molecule.

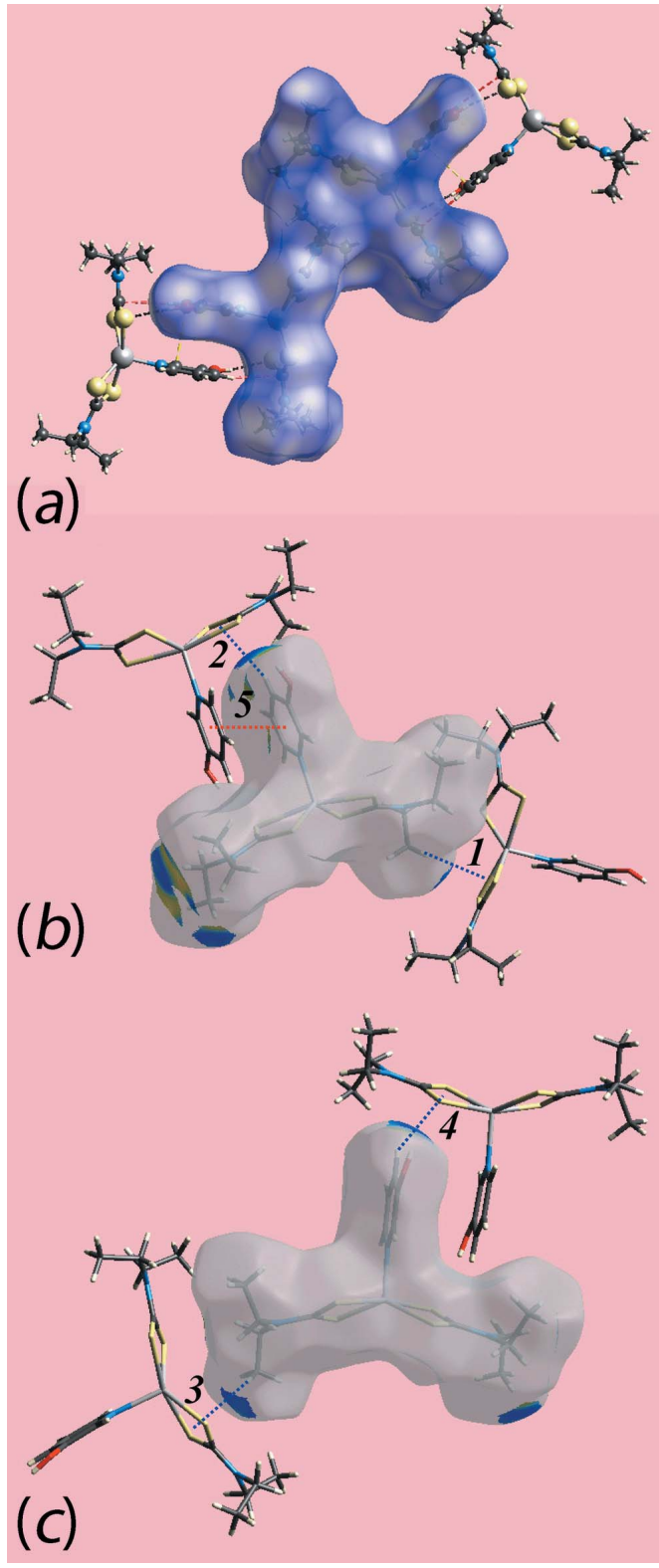

Figure 8
(*a*) View of the Hirshfeld surface mapped over d_{norm} for (I) showing O—H···S hydrogen bonds and short interatomic C···C and C···H/H···C contacts, indicated by black, white and red dashed lines, respectively, about the reference molecule. (*b*) and (*c*) Views of Hirshfeld surface mapped with shape-index property about the Zn1 and Zn2-containing molecules, respectively. The dotted blue lines labelled with 1-4 indicates C—H···π(chelate) interactions and the red dotted line shows the π–π stacking interaction.

immediate environments around reference molecules showing above intermolecular interactions are illustrated in Fig. 8.

The presence of peripheral hydroxy groups participating in the O—H···O hydrogen bonds in the structure of (II) result in the distinct bright-red spots near the respective donors and acceptor atoms on the Hirshfeld surface mapped over d_{norm}, Fig. 9*a* and 9*b*, and result in the blue and red regions corresponding to positive and negative potential on the Hirshfeld surface mapped over electrostatic potential (mapped over the range −0.12 to +0.18 au), Fig. 9*c*. The faint-red spots near the S4, C8, C9 and H2*B* atoms in Fig. 9*a* and 9*b* indicate their involvement in short interatomic S···S, C···C and C···H/H···C contacts, Table 4. Fig. 10*a* illustrates the immediate environment about a reference molecule within Hirshfeld surfaces mapped over electrostatic potential and highlights the O—H···O hydrogen bonds. The C—H···π(chelate) and its reciprocal contact, *i.e.* π—H···C, and short interatomic S···S, C···C and C···H/H···C contacts, with labels 3–6, are shown in Fig. 10*b*.

The overall two-dimensional fingerprint plot for individual Zn1- and Zn2-containing molecules, overall (I) and (II) are illustrated in Fig. 11*a*. The respective plots delineated into H···H, O···H/H···O, S···H/H···S, C···H/H···C, C···C and S···S contacts (McKinnon *et al.*, 2007) are shown in Fig. 11*b*–*g*, respectively; the relative contributions from different contacts to the Hirshfeld surfaces of (I) and (II) are summarized in Table 5.

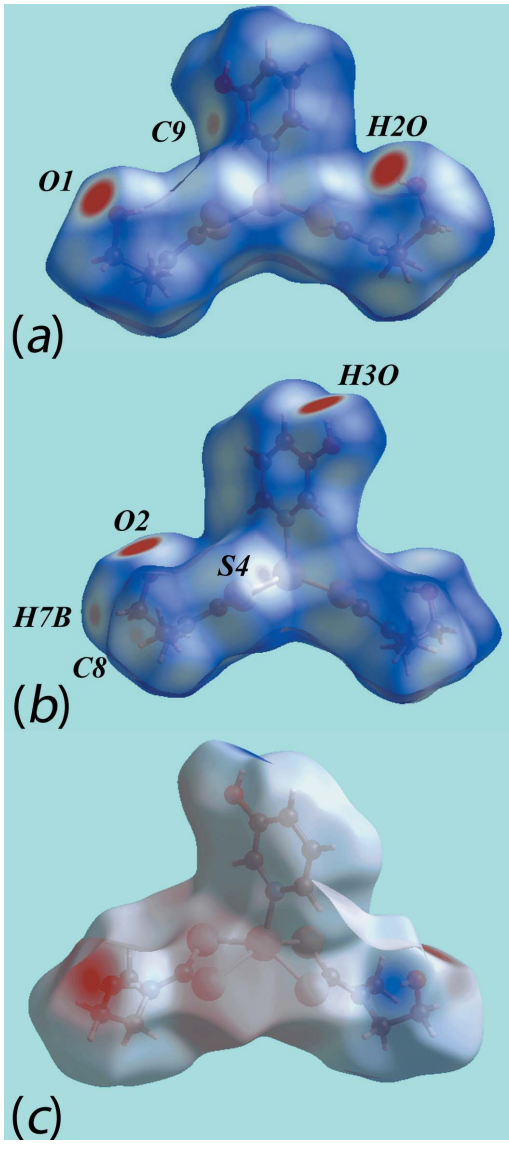

Figure 9
Views of the Hirshfeld surfaces for (II) mapped over (*a*) and (*b*) d_{norm} and (*c*) electrostatic potential.

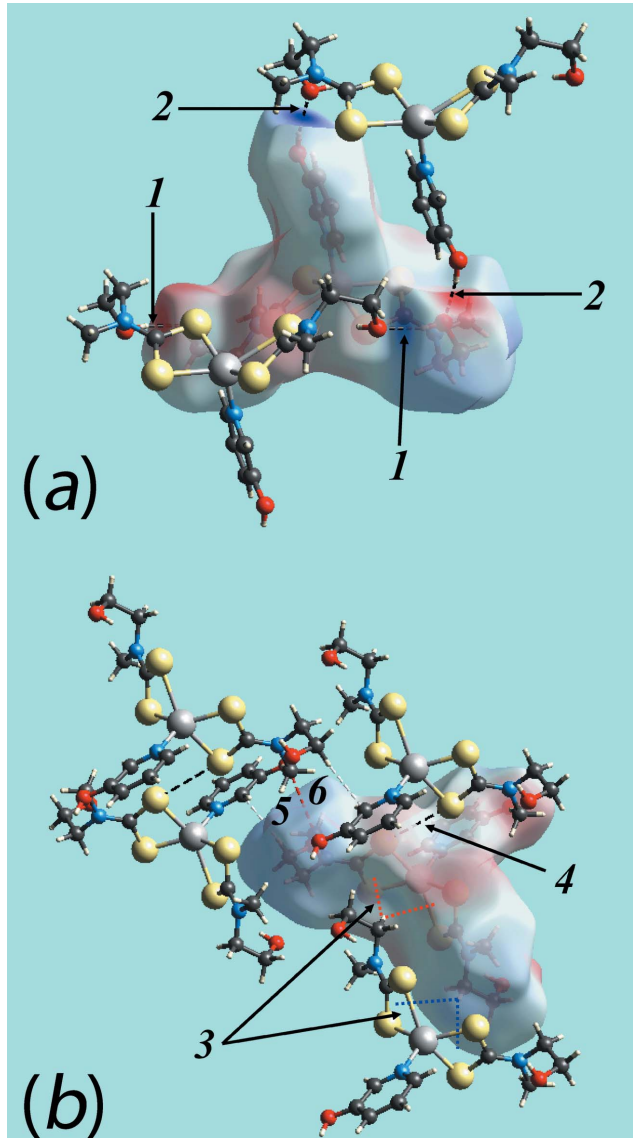

Figure 10
(*a*) and (*b*) Views of the Hirshfeld surface mapped over electrostatic potential for (II) showing O—H···S hydrogen bonds about the reference molecule. The hydrogen bonds are indicated with black dashed lines and labelled as '1' and '2' in (*a*). In (*b*), the intermolecular C—H···O (labelled with a '6' and shown as red-dashed lines) and C—H···π/π···H—C ('3', red and blue) interactions, and short interatomic S···S ('4', black) and C···H ('5', white) contacts are indicated by arrows.

The fingerprint plots delineated into H···H contacts for (I), Fig. 11*b*, show different distributions of points in the individual plots for Zn1- and Zn2-molecules. This, as well as their different percentage contributions to the Hirshfeld surface, Table 5, confirm their distinct chemical environments. The overall plot is the superimposition of these individual plots with a pair of small peaks, at (d_e, d_i) distances shorter than their van der Waals separations, corresponding to short interatomic H···H contacts, Table 4, between the hydrogen atoms of the Zn1-molecule.

The fingerprint plots delineated into O···H/H···O contacts, Fig. 11*c*, also exhibit slightly different profiles for the independent molecules. The respective peaks at $d_e + d_i \sim 2.7$ Å and ~ 2.6 Å correspond to donors (upper region) and the acceptors (lower region) for the Zn1-molecule, whereas these appear as a pair of peaks at the same $d_e + d_i \sim 2.6$ Å distance for the Zn2-molecule. This is likely due to the interacting oxygen and hydrogen atoms for the Zn1-molecule being at their van der Waals separation in the donor region, *i.e.* at 2.72 Å, while in the acceptor region the peak corresponds to a short interatomic O···H contact, Table 4. In the plot for the Zn2-molecule, this contact gives rise to the pair of peaks at $d_e + d_i \sim 2.6$ Å.

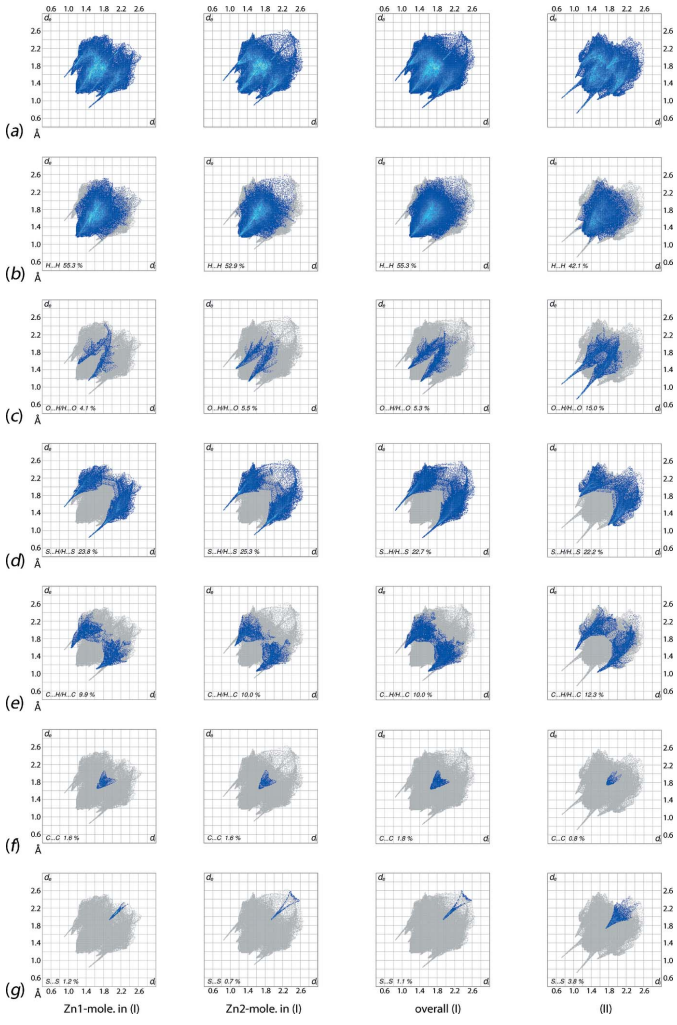

Figure 11
(*a*) The overall two-dimensional fingerprint plots for the Zn1-molecule in (I), Zn2-molecule in (I), (I) and (II), respectively, and those delineated into (*b*) H···H, (*c*) O···H/H···O, (*d*) S···H/H···S, (e) C···H/H···C, (f) C···C and (g) S···S contacts.

Table 5
Percentage contribution to interatomic contacts from the Hirshfeld surface for (I) and (II).

Contact	Zn1-molecule in (I)	Zn2-molecule in (I)	(I)	(II)
H···H	55.3	52.9	55.3	42.1
O···H/H···O	4.1	5.5	5.3	15.0
S···H/H···S	23.8	25.3	22.7	22.2
C···H/H···C	9.9	10.0	10.0	12.3
N···H/H···N	2.6	2.5	2.7	2.9
S···S	1.2	0.7	1.1	3.8
C···C	1.6	1.6	1.8	0.8
Zn···H/H···Zn	0.8	0.8	0.4	0.7
C···O/O···C	0.4	0.4	0.4	0.0
C···N/N···C	0.2	0.2	0.3	0.1
S···O/O···S	0.1	0.1	0.0	0.0
S···C/C···S	0.0	0.0	0.0	0.1

The pair of spikes with their tips at different $d_e + d_i$ distances in the fingerprint plots delineated into S···H/H···S contacts, Fig. 11*d*, for the Zn1- and Zn2-molecules result from different hydroxy-O—H···S(dithiocarbamate) hydrogen bonds. The tips at $d_e + d_i \sim 2.4$ Å in the donor region of the plot for the Zn1-molecule and in the acceptor region for the Zn2-molecule are due to the formation of O—H···S hydrogen bonds between the hydroxy-O1 and dithiocarbamate-S8 atoms; the other hydrogen bond, involving the O2 and S2 atoms, gives rise to tips at $d_e + d_i \sim 2.3$ Å in the respective donor and acceptor regions of the plots, Fig. 11*d*. The plot for the overall structure results from the superimposition of individual plots and shows the symmetric distribution of points as a pair of long spikes having tips at $d_e + d_i \sim 2.3$ Å. The short interatomic S···H/H···S contacts in the crystal of (I), Table 4, appear as a pair of aligned green points beginning at $d_e + d_i \sim 3.0$ Å in the respective plots.

Almost the same percentage contribution from C···H/H···C contacts to the overall surface is made by the Zn1- and Zn2-molecules, Table 5, and the respective fingerprint plots, Fig. 11*e*, have the same shape with tips at $d_e + d_i \sim 2.7$ Å which are due to the short interatomic C···H/H···C contacts, Table 4, involving the atoms forming the C—H···π(chelate) interactions; the points corresponding to the other short C···H/H···C contacts are within the plot. The C···C contacts assigned to intra-dimer π–π stacking interactions between pyOH-rings have a small, *i.e.* 1.8%, but recognizable contribution to the Hirshfeld surface and appear as an arrow-like distribution of points around $d_e = d_i = 1.8$ Å in Fig. 11*f*. As indicated in Fig. 11*g*, S···S contacts do not figure prominently in the molecular packing of (I).

The corresponding two-dimensional fingerprint plots for (II) are also given in Fig. 11. In the fingerprint plots delineated into H···H contacts, Fig. 11*b*, a pair of very thin spikes having their tips at $d_e + d_i \sim 2.3$ Å indicate the presence of short interatomic H···H contacts between hydroxy-H1*O* and -H2*O* atoms, Table 4. Also, the intermolecular O—H···O hydrogen

Table 6
Experimental details.

	(I)	(II)
Crystal data		
Chemical formula	$[Zn(C_5H_{10}NS_2)_2(C_5H_5NO)]$	$[Zn(C_4H_8NOS_2)_2(C_5H_5NO)]$
M_r	456.99	460.94
Crystal system, space group	Monoclinic, $P2_1/c$	Triclinic, $P\overline{1}$
Temperature (K)	98	98
a, b, c (Å)	10.032 (2), 31.955 (7), 13.233 (3)	8.8645 (19), 9.956 (2), 11.473 (3)
α, β, γ (°)	90, 105.920 (2), 90	102.154 (4), 106.989 (4), 93.466 (3)
V (Å^3)	4079.4 (15)	938.6 (4)
Z	8	2
Radiation type	Mo $K\alpha$	Mo $K\alpha$
μ (mm^{-1})	1.62	1.77
Crystal size (mm)	0.50 × 0.40 × 0.15	0.37 × 0.25 × 0.25
Data collection		
Diffractometer	Rigaku AFC12κ/SATURN724	Rigaku AFC12κ/SATURN724
Absorption correction	Multi-scan (*ABSCOR*; Higashi, 1995)	Multi-scan (*ABSCOR*; Higashi, 1995)
T_{min}, T_{max}	0.687, 1.000	0.860, 1.000
No. of measured, independent and observed [$I > 2\sigma(I)$] reflections	25139, 9202, 8401	6836, 4249, 4133
R_{int}	0.037	0.026
(sin $\theta/\lambda)_{max}$ (Å^{-1})	0.650	0.650
Refinement		
$R[F^2 > 2\sigma(F^2)]$, $wR(F^2)$, S	0.041, 0.106, 1.06	0.032, 0.080, 1.06
No. of reflections	9202	4249
No. of parameters	447	228
No. of restraints	2	3
$\Delta\rho_{max}$, $\Delta\rho_{min}$ (e Å^{-3})	0.73, −0.45	0.43, −0.60

Computer programs: *CrystalClear* (Molecular Structure Corporation & Rigaku, 2005), *SHELXS97* (Sheldrick, 2008), *SHELXL2014* (Sheldrick, 2015), *ORTEP-3 for Windows* (Farrugia, 2012), *QMol* (Gans & Shalloway, 2001), *DIAMOND* (Brandenburg, 2006) and *publCIF* (Westrip, 2010).

bond between the pyOH-O3 and hydroxy-O2 atoms results in a short interatomic H···H contact between the H2*O* and H3*O* atoms, Table 4. The increase in the percentage contribution from O···H/H···O contacts to the Hirshfeld surface and the corresponding decrease in the contribution from H···H contacts in (II), *cf.* (I), Table 5, is due to the presence of dominating O—H···O hydrogen bonds in the crystal of (II) and is characterized as a pair of long spikes terminating at $d_e + d_i \sim 1.8$ Å, Fig. 11*c*. The tips corresponding to the O1···H6*A* contact, Table 4, are diminished within the long spikes corresponding to dominant O—H···O hydrogen bonds.

The S···H/H···S contacts with the nearly same contribution to the surface of (II) as for (I), *i.e.* 22.2 and 22.7%, respectively, reflect the O—H···S hydrogen bonds and additional S···H contacts resulting in tips at $d_e + d_i \sim 2.9$ Å in Fig. 11*d* and Table 4. The 12.3% contribution from C···H/H···C contacts to the surface with the tips at $d_e + d_i \sim 2.6$ Å in the plot, Fig. 11*e*, results from the C—H···π(chelate) and short interatomic C···H/H···C contacts, Table 4. The presence of C—H···π(chelate) interactions is also indicated by the short interatomic Zn···H/H···Zn contacts summarized in Table 4. The presence of short interatomic C···C contacts between symmetry-related methyl-C8 atoms is identified in the respective plot, Fig. 11*f*, as the pair of tips at $d_e + d_i \sim 1.7$ Å. Finally, a cone-shaped distribution of points with a 3.8% contribution to the surface from S···S contacts having a vertex at $d_e = d_i \sim 1.7$ Å in the fingerprint plot, Fig. 11*g*, results from short interatomic contacts between S4 atoms, Table 4; the absence of analogous contacts in (I) results in a very low percentage contribution to its surface (see above).

5. Database survey

As alluded to in the *Chemical context*, the presence of hydroxyethyl groups in zinc dithiocarbamates leads to a higher degree of recognizable supramolecular aggregation owing to hydrogen bonding, usually of the type hydroxy-O—H···O(hydroxy) but, sometimes also of the type hydroxy-O—H···S(dithiocarbamate) (Tan *et al.*, 2013; Jamaludin *et al.*, 2016). The following is a brief overview of some previous structures with ethylhydroxydithiocarbamate ligands highlighting the important role of hydrogen bonding in the supramolecular aggregation. In the what might be termed the parent binary compound, *i.e.* $\{Zn[S_2CN(CH_2CH_2OH)_2]_2\}_2$, the usual dimeric motif is evident but these self-assemble *via* strong hydrogen bonding into three-dimensional architectures in both of the polymorphs characterized thus far, with the difference between the structures being the topology of supramolecular layers, *i.e.* flattened (Manohar *et al.*, 1998) and undulating (Benson *et al.*, 2007). When one ethylhydroxy group is replaced by an ethyl group, as in $\{Zn[S_2CN(Et)CH_2CH_2OH]_2\}_2$, the reduced hydrogen bonding leads to supramolecular chains (Benson *et al.*, 2007). Bridging ligands lead to zero-dimensional aggregates, *e.g.* in $\{Zn[S_2CN(Me)CH_2CH_2OH)_2]_2\}_2L$, where L is (3-pyridyl)-$CH_2N(H)C(=O)C(=O)N(H)CH_2$(3-pyridyl). However,

hydrogen bonding of the type hydroxy-O—H···O(hydroxy) links the molecules into inter-woven double chains (Poplaukhin & Tiekink, 2008). The interesting structural chemistry is complimented by observations that some of these compounds exhibit exciting, cell-specific, anti-cancer potential (Tan *et al.*, 2015). The foregoing suggests this is a fertile area of research, well deserving of continuing attention.

6. Synthesis and crystallization

Synthesis of (I): In a 2:1:0.5 molar ratio, $Zn(S_2CNEt_2)_2$, *N*,*N*′-bis(pyridin-3-ylmethyl)ethanedithiodiamide (Zukerman-Schpector *et al.*, 2015) and 3-hydroxy pyridine were dissolved in chloroform. Solvent diffusion of hexane into this solution produced pink crystals. FT–IR (cm^{-1}): ν(C═N) 1482 (*s*, *br*); ν(C—S) 987 (*s*). ^{1}H NMR (d_6-DMSO, 300 MHz): δ 9.91 (*s*, 1H, OH), 8.20–8.00 (*m*, 2H, aromatic-H), 7.30–7.10 (*m*, 2H, aromatic-H), 3.82 (8H, *q*, NCH_2, J = 7.00 Hz); 1.22 (12H, *t*, CH_3, J = 7.20 Hz).

Synthesis of (II): In a 1:1 molar ratio, $Zn[S_2N(Me)CH_2CH_2OH]_2$ and 3-hydroxy pyridine were dissolved in a MeOH/EtOH (1:1 *v*/*v*) solution. Solvent diffusion of hexane into this solution led to the formation of colourless crystals. FT–IR (cm^{-1}): ν(C═N) 1480 (*s*); ν(C—S) 1002 (*s*). ^{1}H NMR (d_6-DMSO, 300 MHz): δ 9.91 (*s*, 1H, aromatic-OH), 8.20–8.00 (*m*, 2H, aromatic-H), 7.30–7.10 (*m*, 2H, aromatic-H), 4.91 (2H, *t*, OH, J = 5.50 Hz); 3.90 (4H, *t*, NCH_2, J = 6.25 Hz); 3.70 (4H, *dt*, CH_2O, J = 5.50, 5.50 Hz); 3.41 (6H, *s*, CH_3).

7. Refinement details

Crystal data, data collection and structure refinement details are summarized in Table 6. The carbon-bound H-atoms were placed in calculated positions (C—H = 0.95–0.99 Å) and were included in the refinement in the riding-model approximation, with U_{iso}(H) set to 1.2–1.5U_{eq}(C). The oxygen-bound H-atoms were located in difference Fourier maps but were refined with a distance restraint of O—H = 0.84±0.01 Å, and with U_{iso}(H) set to 1.5U_{eq}(O).

Acknowledgements

We thank Sunway University for support of biological and crystal engineering studies of metal dithiocarbamates.

References

Addison, A. W., Rao, T. N., Reedijk, J., van Rijn, J. & Verschoor, G. C. (1984). *J. Chem. Soc. Dalton Trans.* pp. 1349–1356.
Benson, R. E., Ellis, C. A., Lewis, C. E. & Tiekink, E. R. T. (2007). *CrystEngComm*, **9**, 930–941.
Bonamico, M., Mazzone, G., Vaciago, A. & Zambonelli, L. (1965). *Acta Cryst.* **19**, 898–909.
Brandenburg, K. (2006). *DIAMOND*. Crystal Impact GbR, Bonn, Germany.
Cardoso, L. N. F., Nogueira, T. C. M., Wardell, J. L., Wardell, S. M. S. V., de Souza, M. V. N., Jotani, M. M. & Tiekink, E. R. T. (2016). *Acta Cryst.* E**72**, 1025–1031.
Cox, M. J. & Tiekink, E. R. T. (2009). *Z. Kristallogr*. **214**, 184–190.
Farrugia, L. J. (2012). *J. Appl. Cryst.* **45**, 849–854.
Gans, J. & Shalloway, D. (2001). *J. Mol. Graphics Modell.* **19**, 557–559.
Heard, P. J. (2005). *Prog. Inorg. Chem*. **53**, 1–69.
Higashi, T. (1995). *ABSCOR*. Rigaku Corporation, Tokyo, Japan.
Ivanov, A. V., Korneeva, E. V., Gerasimenko, A. V. & Forsling, W. (2005). *Russ. J. Coord. Chem.* **31**, 695–707.
Jamaludin, N. S., Halim, S. N. A., Khoo, C.-H., Chen, B.-J., See, T.-H., Sim, J.-H., Cheah, Y.-K., Seng, H.-L. & Tiekink, E. R. T. (2016). *Z. Kristallogr*. **231**, 341–349.
Jotani, M. M., Tan, Y. S. & Tiekink, E. R. T. (2016). *Z. Kristallogr*. **231**, 403–413.
Kang, J.-G., Shin, J.-S., Cho, D.-H., Jeong, Y.-K., Park, C., Soh, S. F., Lai, C. S. & Tiekink, E. R. T. (2010). *Cryst. Growth Des.* **10**, 1247–1256.
Lai, C. S. & Tiekink, E. R. T. (2003). *Appl. Organomet. Chem.* **17**, 251–252.
Malik, M. A., Motevalli, M., O'Brien, P. & Walsh, J. R. (1997). *Inorg. Chem.* **36**, 1263–1264.
Manohar, A., Venkatachalam, V., Ramalingam, K., Thirumaran, S., Bocelli, G. & Cantoni, A. (1998). *J. Chem. Crystallogr.* **28**, 861–866.
McKinnon, J. J., Jayatilaka, D. & Spackman, M. A. (2007). *Chem. Commun*. pp. 3814–3816.
Molecular Structure Corporation & Rigaku (2005). *CrystalClear*. MSC, The Woodlands, Texas, USA, and Rigaku Corporation, Tokyo, Japan.
Poplaukhin, P. & Tiekink, E. R. T. (2008). *Acta Cryst.* E**64**, m1176.
Safbri, S. A. M., Halim, S. N. A. & Tiekink, E. R. T. (2016). *Acta Cryst.* E**72**, 203–208.
Sheldrick, G. M. (2008). *Acta Cryst.* A**64**, 112–122.
Sheldrick, G. M. (2015). *Acta Cryst.* C**71**, 3–8.
Spek, A. L. (2009). *Acta Cryst.* D**65**, 148–155.
Tan, Y. S., Halim, S. N. A., Molloy, K. C., Sudlow, A. L., Otero-de-la-Roza, A. & Tiekink, E. R. T. (2016*a*). *CrystEngComm*, **18**, 1105–1117.
Tan, Y. S., Halim, S. N. A. & Tiekink, E. R. T. (2016*b*). *Z. Kristallogr*. **231**, 113–126.
Tan, Y. S., Ooi, K. K., Ang, K. P., Akim, A. M., Cheah, Y.-K., Halim, S. N. A., Seng, H.-L. & Tiekink, E. R. T. (2015). *J. Inorg. Biochem.* **150**, 48–62.
Tan, Y. S., Sudlow, A. L., Molloy, K. C., Morishima, Y., Fujisawa, K., Jackson, W. J., Henderson, W., Halim, S. N. B. A., Ng, S. W. & Tiekink, E. R. T. (2013). *Cryst. Growth Des.* **13**, 3046–3056.
Tiekink, E. R. T. (2000). *Z. Kristallogr. - New Cryst. Struct*. **215**, 445–446.
Tiekink, E. R. T. (2003). *CrystEngComm*, **5**, 101–113.
Tiekink, E. R. T. & Zukerman-Schpector, J. (2011). *Chem. Commun.* **47**, 6623–6625.
Westrip, S. P. (2010). *J. Appl. Cryst.* **43**, 920–925.
Zeng, D., Hampden-Smith, M. J. & Larson, E. M. (1994). *Acta Cryst.* C**50**, 1000–1002.
Zha, M.-Q., Li, X., Bing, Y. & Lu, Y. (2010). *Acta Cryst.* E**66**, m1465.
Zukerman-Schpector, J., Sousa Madureira, L., Poplaukhin, P., Arman, H. D., Miller, T. & Tiekink, E. R. T. (2015). *Z. Kristallogr*. **230**, 531–541.

supporting information

Acta Cryst. (2016). E**72**, 1700-1709 [https://doi.org/10.1107/S205698901601728X]

Bis(*N*,*N*-diethyldithiocarbamato-κ^2S,S')(3-hydroxypyridine-κN)zinc and bis-[*N*-(2-hydroxyethyl)-*N*-methyldithiocarbamato-κ^2S,S'](3-hydroxypyridine-κN)zinc: crystal structures and Hirshfeld surface analysis

Mukesh M. Jotani, Hadi D. Arman, Pavel Poplaukhin and Edward R. T. Tiekink

Computing details

For both compounds, data collection: *CrystalClear* (Molecular Structure Corporation & Rigaku, 2005); cell refinement: *CrystalClear* (Molecular Structure Corporation & Rigaku, 2005); data reduction: *CrystalClear* (Molecular Structure Corporation & Rigaku, 2005); program(s) used to solve structure: *SHELXS97* (Sheldrick, 2008); program(s) used to refine structure: *SHELXL2014* (Sheldrick, 2015). Molecular graphics: *ORTEP-3 for Windows* (Farrugia, 2012), *QMol* (Gans & Shalloway, 2001), *DIAMOND* (Brandenburg, 2006) for (I); *ORTEP-3 for Windows* (Farrugia, 2012) and *DIAMOND* (Brandenburg, 2006) for (II). For both compounds, software used to prepare material for publication: *publCIF* (Westrip, 2010).

(I) Bis(*N*,*N*-diethyldithiocarbamato-κ^2S,S')(3-hydroxypyridine-κN)zinc

Crystal data

$[Zn(C_5H_{10}NS_2)_2(C_5H_5NO)]$
M_r = 456.99
Monoclinic, $P2_1/c$
a = 10.032 (2) Å
b = 31.955 (7) Å
c = 13.233 (3) Å
β = 105.920 (2)°
V = 4079.4 (15) Å^3
Z = 8
$F(000)$ = 1904
D_x = 1.488 Mg m^{-3}
Mo $K\alpha$ radiation, λ = 0.71073 Å
Cell parameters from 16430 reflections
θ = 2.5–40.7°
μ = 1.62 mm^{-1}
T = 98 K
Slab, pink
0.50 × 0.40 × 0.15 mm

Data collection

Rigaku AFC12κ/SATURN724 diffractometer
Radiation source: fine-focus sealed tube
Graphite monochromator
ω scans
Absorption correction: multi-scan (ABSCOR; Higashi, 1995)
T_{min} = 0.687, T_{max} = 1.000
25139 measured reflections
9202 independent reflections
8401 reflections with $I > 2\sigma(I)$
R_{int} = 0.037
θ_{max} = 27.5°, θ_{min} = 2.5°
h = −10→13
k = −41→41
l = −17→17

Refinement

Refinement on F^2
Least-squares matrix: full
$R[F^2 > 2\sigma(F^2)] = 0.041$
$wR(F^2) = 0.106$
$S = 1.06$
9202 reflections
447 parameters
2 restraints

Primary atom site location: structure-invariant direct methods
Secondary atom site location: difference Fourier map
Hydrogen site location: mixed
$w = 1/[\sigma^2(F_o^2) + (0.0477P)^2 + 4.2267P]$ where $P = (F_o^2 + 2F_c^2)/3$
$(\Delta/\sigma)_{max} = 0.002$
$\Delta\rho_{max} = 0.73$ e Å^{-3}
$\Delta\rho_{min} = -0.45$ e Å^{-3}

Special details

Geometry. All esds (except the esd in the dihedral angle between two l.s. planes) are estimated using the full covariance matrix. The cell esds are taken into account individually in the estimation of esds in distances, angles and torsion angles; correlations between esds in cell parameters are only used when they are defined by crystal symmetry. An approximate (isotropic) treatment of cell esds is used for estimating esds involving l.s. planes.

Fractional atomic coordinates and isotropic or equivalent isotropic displacement parameters (Å²)

	x	*y*	*z*	U_{iso}*/U_{eq}
Zn1	0.22939 (3)	0.51145 (2)	0.27529 (3)	0.02233 (8)
S1	0.06711 (7)	0.51485 (2)	0.37067 (5)	0.02470 (14)
S2	−0.01500 (6)	0.54220 (2)	0.14827 (5)	0.02127 (13)
S3	0.27656 (6)	0.46663 (2)	0.14937 (5)	0.02206 (13)
S4	0.42106 (7)	0.46582 (2)	0.37705 (5)	0.02349 (14)
O1	0.5087 (2)	0.64627 (6)	0.45759 (17)	0.0305 (4)
H1O	0.524 (4)	0.6717 (4)	0.449 (3)	0.046*
N1	−0.1829 (2)	0.54510 (7)	0.27436 (17)	0.0206 (4)
N2	0.4941 (2)	0.41780 (7)	0.23507 (18)	0.0218 (4)
N3	0.3333 (2)	0.56740 (7)	0.27551 (18)	0.0209 (4)
C1	−0.0580 (3)	0.53538 (8)	0.2645 (2)	0.0194 (5)
C2	−0.2190 (3)	0.54050 (9)	0.3748 (2)	0.0257 (5)
H2A	−0.1631	0.5176	0.4162	0.031*
H2B	−0.3180	0.5327	0.3602	0.031*
C3	−0.1933 (3)	0.58063 (10)	0.4389 (2)	0.0339 (7)
H3A	−0.0933	0.5856	0.4649	0.051*
H3B	−0.2330	0.5780	0.4985	0.051*
H3C	−0.2371	0.6041	0.3946	0.051*
C4	−0.2961 (3)	0.55989 (9)	0.1855 (2)	0.0265 (5)
H4A	−0.2567	0.5750	0.1350	0.032*
H4B	−0.3553	0.5796	0.2114	0.032*
C5	−0.3837 (3)	0.52333 (10)	0.1301 (2)	0.0334 (6)
H5A	−0.3275	0.5054	0.0978	0.050*
H5B	−0.4634	0.5340	0.0756	0.050*
H5C	−0.4166	0.5071	0.1813	0.050*
C6	0.4075 (3)	0.44668 (8)	0.2532 (2)	0.0203 (5)
C7	0.4939 (3)	0.40561 (9)	0.1276 (2)	0.0268 (6)
H7A	0.5897	0.3983	0.1272	0.032*
H7B	0.4644	0.4299	0.0804	0.032*

C8	0.3997 (3)	0.36900 (10)	0.0850 (3)	0.0353 (7)
H8A	0.4218	0.3457	0.1350	0.053*
H8B	0.4134	0.3602	0.0177	0.053*
H8C	0.3030	0.3774	0.0748	0.053*
C9	0.6003 (3)	0.39774 (8)	0.3208 (2)	0.0261 (5)
H9A	0.6182	0.3691	0.2992	0.031*
H9B	0.5651	0.3954	0.3836	0.031*
C10	0.7353 (3)	0.42242 (10)	0.3491 (2)	0.0313 (6)
H10A	0.7667	0.4266	0.2860	0.047*
H10B	0.8060	0.4069	0.4015	0.047*
H10C	0.7201	0.4497	0.3782	0.047*
C11	0.3950 (3)	0.58787 (8)	0.3647 (2)	0.0236 (5)
H11	0.4004	0.5749	0.4303	0.028*
C12	0.4514 (3)	0.62776 (8)	0.3636 (2)	0.0236 (5)
C13	0.4457 (3)	0.64633 (8)	0.2680 (2)	0.0242 (5)
H13	0.4834	0.6734	0.2653	0.029*
C14	0.3839 (3)	0.62468 (9)	0.1761 (2)	0.0266 (5)
H14	0.3798	0.6366	0.1096	0.032*
C15	0.3287 (3)	0.58556 (9)	0.1827 (2)	0.0233 (5)
H15	0.2859	0.5709	0.1197	0.028*
Zn2	0.68820 (3)	0.27217 (2)	0.19561 (3)	0.02217 (8)
S5	0.75317 (6)	0.32449 (2)	0.09483 (5)	0.02196 (13)
S6	0.89261 (7)	0.30961 (2)	0.31945 (5)	0.02480 (14)
S7	0.52971 (7)	0.26483 (2)	0.29651 (5)	0.02464 (14)
S8	0.45448 (6)	0.24765 (2)	0.06815 (5)	0.02173 (13)
O2	0.9810 (2)	0.13960 (6)	0.36656 (16)	0.0293 (4)
H2O	0.997 (4)	0.1141 (4)	0.358 (3)	0.044*
N4	0.9764 (2)	0.36702 (7)	0.20279 (18)	0.0214 (4)
N5	0.2806 (2)	0.23709 (7)	0.18746 (18)	0.0218 (4)
N6	0.7917 (2)	0.21685 (7)	0.18654 (18)	0.0214 (4)
C16	0.8854 (3)	0.33725 (8)	0.2066 (2)	0.0196 (5)
C17	1.0857 (3)	0.37985 (9)	0.2973 (2)	0.0270 (6)
H17A	1.0512	0.3764	0.3601	0.032*
H17B	1.1075	0.4098	0.2914	0.032*
C18	1.2165 (3)	0.35417 (10)	0.3110 (3)	0.0358 (7)
H18A	1.1964	0.3247	0.3211	0.054*
H18B	1.2880	0.3642	0.3725	0.054*
H18C	1.2497	0.3570	0.2482	0.054*
C19	0.9748 (3)	0.38995 (8)	0.1058 (2)	0.0246 (5)
H19A	0.9319	0.3722	0.0442	0.030*
H19B	1.0713	0.3959	0.1050	0.030*
C20	0.8951 (3)	0.43075 (9)	0.0970 (2)	0.0284 (6)
H20A	0.7968	0.4248	0.0881	0.043*
H20B	0.9056	0.4466	0.0362	0.043*
H20C	0.9315	0.4473	0.1610	0.043*
C21	0.4063 (3)	0.24864 (8)	0.1840 (2)	0.0206 (5)
C22	0.2413 (3)	0.23388 (9)	0.2868 (2)	0.0247 (5)
H22A	0.1416	0.2405	0.2736	0.030*

H22B	0.2948	0.2546	0.3377	0.030*
C23	0.2691 (3)	0.19034 (10)	0.3332 (2)	0.0310 (6)
H23A	0.2249	0.1696	0.2800	0.047*
H23B	0.2311	0.1879	0.3937	0.047*
H23C	0.3693	0.1853	0.3559	0.047*
C24	0.1702 (3)	0.22577 (9)	0.0921 (2)	0.0262 (6)
H24A	0.1135	0.2028	0.1086	0.031*
H24B	0.2125	0.2158	0.0371	0.031*
C25	0.0776 (3)	0.26349 (11)	0.0511 (3)	0.0371 (7)
H25A	0.0353	0.2732	0.1053	0.056*
H25B	0.0047	0.2554	−0.0118	0.056*
H25C	0.1335	0.2860	0.0333	0.056*
C26	0.8547 (3)	0.19591 (8)	0.2743 (2)	0.0225 (5)
H26	0.8552	0.2078	0.3402	0.027*
C27	0.9194 (3)	0.15755 (8)	0.2729 (2)	0.0223 (5)
C28	0.9185 (3)	0.14053 (8)	0.1761 (2)	0.0249 (5)
H28	0.9612	0.1143	0.1720	0.030*
C29	0.8541 (3)	0.16261 (9)	0.0855 (2)	0.0261 (5)
H29	0.8533	0.1517	0.0185	0.031*
C30	0.7912 (3)	0.20054 (9)	0.0932 (2)	0.0242 (5)
H30	0.7466	0.2154	0.0308	0.029*

Atomic displacement parameters (Å²)

	U^{11}	U^{22}	U^{33}	U^{12}	U^{13}	U^{23}
Zn1	0.02198 (15)	0.01845 (15)	0.02877 (17)	−0.00025 (11)	0.01071 (12)	−0.00238 (12)
S1	0.0212 (3)	0.0328 (3)	0.0206 (3)	0.0046 (2)	0.0065 (2)	0.0053 (3)
S2	0.0235 (3)	0.0222 (3)	0.0186 (3)	−0.0006 (2)	0.0066 (2)	−0.0003 (2)
S3	0.0209 (3)	0.0226 (3)	0.0217 (3)	0.0009 (2)	0.0042 (2)	−0.0024 (2)
S4	0.0270 (3)	0.0237 (3)	0.0202 (3)	0.0043 (2)	0.0073 (2)	−0.0009 (2)
O1	0.0391 (11)	0.0230 (10)	0.0248 (10)	−0.0026 (8)	0.0011 (9)	−0.0029 (8)
N1	0.0190 (10)	0.0225 (10)	0.0192 (11)	0.0006 (8)	0.0032 (8)	0.0007 (8)
N2	0.0232 (10)	0.0208 (10)	0.0222 (11)	0.0011 (8)	0.0074 (9)	−0.0022 (8)
N3	0.0192 (10)	0.0210 (10)	0.0222 (11)	0.0010 (8)	0.0052 (8)	0.0012 (8)
C1	0.0226 (12)	0.0163 (11)	0.0192 (12)	−0.0006 (9)	0.0054 (9)	−0.0002 (9)
C2	0.0212 (12)	0.0324 (14)	0.0251 (14)	0.0000 (10)	0.0090 (10)	0.0014 (11)
C3	0.0349 (15)	0.0411 (17)	0.0294 (15)	−0.0047 (13)	0.0148 (13)	−0.0096 (13)
C4	0.0208 (12)	0.0296 (14)	0.0270 (14)	0.0024 (10)	0.0031 (10)	0.0054 (11)
C5	0.0261 (13)	0.0419 (17)	0.0280 (15)	−0.0048 (12)	0.0002 (11)	0.0000 (13)
C6	0.0201 (11)	0.0168 (11)	0.0256 (13)	−0.0016 (9)	0.0088 (10)	0.0004 (10)
C7	0.0258 (13)	0.0278 (13)	0.0286 (14)	0.0034 (10)	0.0108 (11)	−0.0057 (11)
C8	0.0338 (15)	0.0347 (16)	0.0362 (17)	−0.0002 (12)	0.0075 (13)	−0.0166 (13)
C9	0.0273 (13)	0.0213 (12)	0.0293 (14)	0.0061 (10)	0.0069 (11)	0.0023 (11)
C10	0.0265 (13)	0.0316 (15)	0.0326 (16)	0.0047 (11)	0.0028 (12)	0.0020 (12)
C11	0.0240 (12)	0.0229 (12)	0.0226 (13)	0.0019 (10)	0.0040 (10)	0.0006 (10)
C12	0.0181 (11)	0.0239 (13)	0.0263 (14)	0.0028 (9)	0.0020 (10)	−0.0041 (10)
C13	0.0223 (12)	0.0202 (12)	0.0312 (15)	−0.0001 (9)	0.0090 (11)	0.0007 (10)
C14	0.0278 (13)	0.0280 (14)	0.0250 (14)	0.0036 (10)	0.0087 (11)	0.0039 (11)

C15	0.0218 (12)	0.0263 (13)	0.0211 (13)	0.0003 (10)	0.0045 (10)	−0.0001 (10)
Zn2	0.02096 (15)	0.01850 (15)	0.02802 (17)	−0.00040 (10)	0.00836 (12)	0.00219 (11)
S5	0.0212 (3)	0.0211 (3)	0.0224 (3)	−0.0027 (2)	0.0039 (2)	0.0019 (2)
S6	0.0299 (3)	0.0234 (3)	0.0208 (3)	−0.0021 (2)	0.0064 (3)	0.0019 (2)
S7	0.0225 (3)	0.0297 (3)	0.0209 (3)	−0.0035 (2)	0.0046 (2)	−0.0031 (3)
S8	0.0221 (3)	0.0229 (3)	0.0200 (3)	−0.0008 (2)	0.0055 (2)	0.0026 (2)
O2	0.0397 (11)	0.0231 (10)	0.0245 (10)	0.0017 (8)	0.0078 (9)	0.0027 (8)
N4	0.0217 (10)	0.0207 (10)	0.0210 (11)	−0.0033 (8)	0.0043 (8)	−0.0025 (8)
N5	0.0224 (10)	0.0221 (10)	0.0209 (11)	0.0000 (8)	0.0059 (9)	0.0010 (9)
N6	0.0186 (10)	0.0204 (10)	0.0247 (11)	−0.0032 (8)	0.0053 (8)	0.0005 (9)
C16	0.0222 (11)	0.0186 (11)	0.0195 (12)	0.0002 (9)	0.0083 (9)	−0.0007 (9)
C17	0.0295 (13)	0.0257 (13)	0.0222 (13)	−0.0072 (10)	0.0010 (11)	−0.0053 (10)
C18	0.0297 (14)	0.0371 (16)	0.0357 (17)	−0.0021 (12)	0.0008 (13)	−0.0001 (13)
C19	0.0286 (13)	0.0251 (13)	0.0223 (13)	−0.0056 (10)	0.0104 (11)	0.0005 (10)
C20	0.0348 (14)	0.0229 (13)	0.0280 (15)	−0.0049 (11)	0.0094 (12)	0.0033 (11)
C21	0.0228 (12)	0.0173 (11)	0.0203 (12)	0.0024 (9)	0.0038 (10)	0.0031 (9)
C22	0.0224 (12)	0.0294 (13)	0.0241 (14)	0.0006 (10)	0.0097 (10)	0.0002 (11)
C23	0.0300 (14)	0.0353 (15)	0.0291 (15)	0.0021 (12)	0.0102 (12)	0.0061 (12)
C24	0.0191 (12)	0.0310 (14)	0.0252 (14)	−0.0042 (10)	0.0006 (10)	−0.0010 (11)
C25	0.0282 (14)	0.0408 (17)	0.0348 (17)	0.0039 (12)	−0.0037 (13)	0.0059 (14)
C26	0.0235 (12)	0.0221 (12)	0.0214 (13)	−0.0022 (9)	0.0052 (10)	−0.0016 (10)
C27	0.0241 (12)	0.0186 (12)	0.0242 (13)	−0.0030 (9)	0.0068 (10)	0.0014 (10)
C28	0.0284 (13)	0.0197 (12)	0.0288 (14)	0.0000 (10)	0.0113 (11)	−0.0013 (10)
C29	0.0335 (14)	0.0259 (13)	0.0200 (13)	−0.0018 (11)	0.0091 (11)	−0.0006 (10)
C30	0.0244 (12)	0.0252 (13)	0.0227 (13)	−0.0014 (10)	0.0063 (10)	0.0038 (10)

Geometric parameters (Å, º)

Zn1—N3	2.069 (2)	Zn2—N6	2.070 (2)
Zn1—S1	2.3201 (8)	Zn2—S5	2.3399 (8)
Zn1—S3	2.3417 (8)	Zn2—S7	2.3517 (8)
Zn1—S4	2.4932 (8)	Zn2—S6	2.5453 (8)
Zn1—S2	2.7461 (8)	Zn2—S8	2.6051 (8)
S1—C1	1.736 (3)	S5—C16	1.743 (3)
S2—C1	1.721 (3)	S6—C16	1.720 (3)
S3—C6	1.741 (3)	S7—C21	1.734 (3)
S4—C6	1.720 (3)	S8—C21	1.730 (3)
O1—C12	1.355 (3)	O2—C27	1.352 (3)
O1—H1O	0.842 (10)	O2—H2O	0.844 (10)
N1—C1	1.332 (3)	N4—C16	1.328 (3)
N1—C4	1.470 (3)	N4—C19	1.474 (3)
N1—C2	1.477 (3)	N4—C17	1.478 (3)
N2—C6	1.333 (3)	N5—C21	1.326 (3)
N2—C9	1.473 (3)	N5—C22	1.476 (3)
N2—C7	1.474 (3)	N5—C24	1.478 (3)
N3—C11	1.343 (3)	N6—C26	1.339 (3)
N3—C15	1.347 (3)	N6—C30	1.340 (4)
C2—C3	1.520 (4)	C17—C18	1.515 (4)

C2—H2A	0.9900	C17—H17A	0.9900
C2—H2B	0.9900	C17—H17B	0.9900
C3—H3A	0.9800	C18—H18A	0.9800
C3—H3B	0.9800	C18—H18B	0.9800
C3—H3C	0.9800	C18—H18C	0.9800
C4—C5	1.524 (4)	C19—C20	1.517 (4)
C4—H4A	0.9900	C19—H19A	0.9900
C4—H4B	0.9900	C19—H19B	0.9900
C5—H5A	0.9800	C20—H20A	0.9800
C5—H5B	0.9800	C20—H20B	0.9800
C5—H5C	0.9800	C20—H20C	0.9800
C7—C8	1.512 (4)	C22—C23	1.515 (4)
C7—H7A	0.9900	C22—H22A	0.9900
C7—H7B	0.9900	C22—H22B	0.9900
C8—H8A	0.9800	C23—H23A	0.9800
C8—H8B	0.9800	C23—H23B	0.9800
C8—H8C	0.9800	C23—H23C	0.9800
C9—C10	1.523 (4)	C24—C25	1.528 (4)
C9—H9A	0.9900	C24—H24A	0.9900
C9—H9B	0.9900	C24—H24B	0.9900
C10—H10A	0.9800	C25—H25A	0.9800
C10—H10B	0.9800	C25—H25B	0.9800
C10—H10C	0.9800	C25—H25C	0.9800
C11—C12	1.397 (4)	C26—C27	1.390 (4)
C11—H11	0.9500	C26—H26	0.9500
C12—C13	1.384 (4)	C27—C28	1.389 (4)
C13—C14	1.388 (4)	C28—C29	1.389 (4)
C13—H13	0.9500	C28—H28	0.9500
C14—C15	1.380 (4)	C29—C30	1.383 (4)
C14—H14	0.9500	C29—H29	0.9500
C15—H15	0.9500	C30—H30	0.9500

N3—Zn1—S1	112.77 (6)	N6—Zn2—S5	110.78 (6)
N3—Zn1—S3	109.24 (6)	N6—Zn2—S7	112.06 (6)
S1—Zn1—S3	136.44 (3)	S5—Zn2—S7	137.08 (3)
N3—Zn1—S4	101.02 (6)	N6—Zn2—S6	96.34 (6)
S1—Zn1—S4	106.61 (3)	S5—Zn2—S6	74.34 (3)
S3—Zn1—S4	75.54 (3)	S7—Zn2—S6	103.42 (3)
N3—Zn1—S2	93.23 (6)	N6—Zn2—S8	94.71 (6)
S1—Zn1—S2	70.99 (3)	S5—Zn2—S8	100.83 (3)
S3—Zn1—S2	95.97 (3)	S7—Zn2—S8	73.08 (3)
S4—Zn1—S2	165.17 (2)	S6—Zn2—S8	168.91 (2)
C1—S1—Zn1	92.11 (9)	C16—S5—Zn2	87.12 (9)
C1—S2—Zn1	78.96 (9)	C16—S6—Zn2	81.24 (9)
C6—S3—Zn1	85.32 (9)	C21—S7—Zn2	88.69 (9)
C6—S4—Zn1	81.11 (9)	C21—S8—Zn2	80.88 (9)
C12—O1—H1O	110 (3)	C27—O2—H2O	110 (3)
C1—N1—C4	122.5 (2)	C16—N4—C19	123.1 (2)

C1—N1—C2	122.3 (2)	C16—N4—C17	121.7 (2)
C4—N1—C2	115.2 (2)	C19—N4—C17	115.3 (2)
C6—N2—C9	122.1 (2)	C21—N5—C22	122.6 (2)
C6—N2—C7	121.9 (2)	C21—N5—C24	122.4 (2)
C9—N2—C7	116.0 (2)	C22—N5—C24	115.0 (2)
C11—N3—C15	118.9 (2)	C26—N6—C30	119.1 (2)
C11—N3—Zn1	122.19 (18)	C26—N6—Zn2	120.10 (18)
C15—N3—Zn1	118.67 (18)	C30—N6—Zn2	120.70 (18)
N1—C1—S2	122.1 (2)	N4—C16—S6	122.3 (2)
N1—C1—S1	119.98 (19)	N4—C16—S5	120.4 (2)
S2—C1—S1	117.91 (14)	S6—C16—S5	117.23 (14)
N1—C2—C3	111.8 (2)	N4—C17—C18	111.6 (2)
N1—C2—H2A	109.2	N4—C17—H17A	109.3
C3—C2—H2A	109.2	C18—C17—H17A	109.3
N1—C2—H2B	109.2	N4—C17—H17B	109.3
C3—C2—H2B	109.2	C18—C17—H17B	109.3
H2A—C2—H2B	107.9	H17A—C17—H17B	108.0
C2—C3—H3A	109.5	C17—C18—H18A	109.5
C2—C3—H3B	109.5	C17—C18—H18B	109.5
H3A—C3—H3B	109.5	H18A—C18—H18B	109.5
C2—C3—H3C	109.5	C17—C18—H18C	109.5
H3A—C3—H3C	109.5	H18A—C18—H18C	109.5
H3B—C3—H3C	109.5	H18B—C18—H18C	109.5
N1—C4—C5	110.8 (2)	N4—C19—C20	111.9 (2)
N1—C4—H4A	109.5	N4—C19—H19A	109.2
C5—C4—H4A	109.5	C20—C19—H19A	109.2
N1—C4—H4B	109.5	N4—C19—H19B	109.2
C5—C4—H4B	109.5	C20—C19—H19B	109.2
H4A—C4—H4B	108.1	H19A—C19—H19B	107.9
C4—C5—H5A	109.5	C19—C20—H20A	109.5
C4—C5—H5B	109.5	C19—C20—H20B	109.5
H5A—C5—H5B	109.5	H20A—C20—H20B	109.5
C4—C5—H5C	109.5	C19—C20—H20C	109.5
H5A—C5—H5C	109.5	H20A—C20—H20C	109.5
H5B—C5—H5C	109.5	H20B—C20—H20C	109.5
N2—C6—S4	122.2 (2)	N5—C21—S8	121.7 (2)
N2—C6—S3	120.0 (2)	N5—C21—S7	121.0 (2)
S4—C6—S3	117.86 (14)	S8—C21—S7	117.32 (15)
N2—C7—C8	113.5 (2)	N5—C22—C23	111.1 (2)
N2—C7—H7A	108.9	N5—C22—H22A	109.4
C8—C7—H7A	108.9	C23—C22—H22A	109.4
N2—C7—H7B	108.9	N5—C22—H22B	109.4
C8—C7—H7B	108.9	C23—C22—H22B	109.4
H7A—C7—H7B	107.7	H22A—C22—H22B	108.0
C7—C8—H8A	109.5	C22—C23—H23A	109.5
C7—C8—H8B	109.5	C22—C23—H23B	109.5
H8A—C8—H8B	109.5	H23A—C23—H23B	109.5
C7—C8—H8C	109.5	C22—C23—H23C	109.5

H8A—C8—H8C	109.5	H23A—C23—H23C	109.5
H8B—C8—H8C	109.5	H23B—C23—H23C	109.5
N2—C9—C10	111.8 (2)	N5—C24—C25	110.5 (2)
N2—C9—H9A	109.3	N5—C24—H24A	109.5
C10—C9—H9A	109.3	C25—C24—H24A	109.5
N2—C9—H9B	109.3	N5—C24—H24B	109.5
C10—C9—H9B	109.3	C25—C24—H24B	109.5
H9A—C9—H9B	107.9	H24A—C24—H24B	108.1
C9—C10—H10A	109.5	C24—C25—H25A	109.5
C9—C10—H10B	109.5	C24—C25—H25B	109.5
H10A—C10—H10B	109.5	H25A—C25—H25B	109.5
C9—C10—H10C	109.5	C24—C25—H25C	109.5
H10A—C10—H10C	109.5	H25A—C25—H25C	109.5
H10B—C10—H10C	109.5	H25B—C25—H25C	109.5
N3—C11—C12	121.7 (3)	N6—C26—C27	122.7 (3)
N3—C11—H11	119.2	N6—C26—H26	118.7
C12—C11—H11	119.2	C27—C26—H26	118.7
O1—C12—C13	123.6 (3)	O2—C27—C28	124.4 (2)
O1—C12—C11	117.4 (3)	O2—C27—C26	117.3 (2)
C13—C12—C11	119.1 (3)	C28—C27—C26	118.3 (3)
C12—C13—C14	118.9 (3)	C27—C28—C29	118.7 (3)
C12—C13—H13	120.5	C27—C28—H28	120.6
C14—C13—H13	120.5	C29—C28—H28	120.6
C15—C14—C13	119.1 (3)	C30—C29—C28	119.7 (3)
C15—C14—H14	120.5	C30—C29—H29	120.2
C13—C14—H14	120.5	C28—C29—H29	120.2
N3—C15—C14	122.3 (3)	N6—C30—C29	121.5 (3)
N3—C15—H15	118.8	N6—C30—H30	119.3
C14—C15—H15	118.8	C29—C30—H30	119.3

C4—N1—C1—S2	3.9 (3)	C19—N4—C16—S6	177.68 (19)
C2—N1—C1—S2	−178.13 (19)	C17—N4—C16—S6	−3.3 (3)
C4—N1—C1—S1	−175.75 (19)	C19—N4—C16—S5	−1.8 (3)
C2—N1—C1—S1	2.2 (3)	C17—N4—C16—S5	177.20 (19)
Zn1—S2—C1—N1	179.1 (2)	Zn2—S6—C16—N4	−177.2 (2)
Zn1—S2—C1—S1	−1.28 (12)	Zn2—S6—C16—S5	2.33 (12)
Zn1—S1—C1—N1	−178.9 (2)	Zn2—S5—C16—N4	177.0 (2)
Zn1—S1—C1—S2	1.49 (14)	Zn2—S5—C16—S6	−2.51 (13)
C1—N1—C2—C3	92.4 (3)	C16—N4—C17—C18	89.7 (3)
C4—N1—C2—C3	−89.5 (3)	C19—N4—C17—C18	−91.2 (3)
C1—N1—C4—C5	91.2 (3)	C16—N4—C19—C20	94.5 (3)
C2—N1—C4—C5	−86.9 (3)	C17—N4—C19—C20	−84.6 (3)
C9—N2—C6—S4	5.1 (3)	C22—N5—C21—S8	174.11 (19)
C7—N2—C6—S4	−171.71 (19)	C24—N5—C21—S8	−4.8 (3)
C9—N2—C6—S3	−175.58 (19)	C22—N5—C21—S7	−5.2 (3)
C7—N2—C6—S3	7.6 (3)	C24—N5—C21—S7	175.93 (19)
Zn1—S4—C6—N2	175.6 (2)	Zn2—S8—C21—N5	−177.8 (2)
Zn1—S4—C6—S3	−3.74 (12)	Zn2—S8—C21—S7	1.50 (12)

Zn1—S3—C6—N2	−175.4 (2)	Zn2—S7—C21—N5	177.7 (2)
Zn1—S3—C6—S4	3.94 (13)	Zn2—S7—C21—S8	−1.64 (14)
C6—N2—C7—C8	−91.5 (3)	C21—N5—C22—C23	−90.3 (3)
C9—N2—C7—C8	91.5 (3)	C24—N5—C22—C23	88.7 (3)
C6—N2—C9—C10	−88.5 (3)	C21—N5—C24—C25	−95.2 (3)
C7—N2—C9—C10	88.5 (3)	C22—N5—C24—C25	85.8 (3)
C15—N3—C11—C12	1.5 (4)	C30—N6—C26—C27	−0.4 (4)
Zn1—N3—C11—C12	−172.77 (19)	Zn2—N6—C26—C27	176.51 (19)
N3—C11—C12—O1	178.6 (2)	N6—C26—C27—O2	179.3 (2)
N3—C11—C12—C13	−1.2 (4)	N6—C26—C27—C28	0.2 (4)
O1—C12—C13—C14	−179.7 (2)	O2—C27—C28—C29	−178.6 (2)
C11—C12—C13—C14	0.0 (4)	C26—C27—C28—C29	0.4 (4)
C12—C13—C14—C15	0.8 (4)	C27—C28—C29—C30	−0.8 (4)
C11—N3—C15—C14	−0.7 (4)	C26—N6—C30—C29	0.1 (4)
Zn1—N3—C15—C14	173.8 (2)	Zn2—N6—C30—C29	−176.88 (19)
C13—C14—C15—N3	−0.4 (4)	C28—C29—C30—N6	0.6 (4)

Hydrogen-bond geometry (Å, º)

Cg1 and Cg2 are the centroids of the (Zn1,S1,S2,C1) and (Zn2,S7,S8,C21) chelate rings, respectively.

D—H···*A*	*D*—H	H···*A*	*D*···*A*	*D*—H···*A*
O1—H1*O*···S8^{i}	0.84 (2)	2.45 (1)	3.289 (2)	173 (4)
O2—H2*O*···S2^{ii}	0.84 (2)	2.31 (1)	3.143 (2)	170 (4)
C8—H8*A*···*Cg*2	0.98	2.98	3.855 (3)	150
C13—H13···*Cg*2^{i}	0.95	2.79	3.631 (3)	148
C20—H20*C*···*Cg*1^{iii}	0.98	2.97	3.850 (3)	150
C28—H28···*Cg*1^{ii}	0.95	2.96	3.738 (3)	140
C19—H19*A*···O2^{iv}	0.99	2.56	3.321 (3)	134

Symmetry codes: (i) −*x*+1, *y*+1/2, −*z*+1/2; (ii) −*x*+1, *y*−1/2, −*z*+1/2; (iii) *x*+1, *y*, *z*; (iv) *x*, −*y*+1/2, *z*−1/2.

(II) Bis[*N*-(2-hydroxyethyl)-*N*-methyldithiocarbamato-κ^2S,S'](3-hydroxypyridine-κN)zinc

Crystal data

$[Zn(C_4H_8NOS_2)_2(C_5H_5NO)]$
M_r = 460.94
Triclinic, $P\overline{1}$
a = 8.8645 (19) Å
b = 9.956 (2) Å
c = 11.473 (3) Å
α = 102.154 (4)°
β = 106.989 (4)°
γ = 93.466 (3)°
V = 938.6 (4) Å^3
Z = 2
F(000) = 476
D_x = 1.631 Mg m^{-3}
Mo *Kα* radiation, *λ* = 0.71073 Å
Cell parameters from 4145 reflections
θ = 2.5–40.6°
μ = 1.77 mm^{-1}
T = 98 K
Slab, colourless
0.37 × 0.25 × 0.25 mm

Data collection

Rigaku AFC12*κ*/SATURN724 diffractometer
Radiation source: fine-focus sealed tube
Graphite monochromator
ω scans
Absorption correction: multi-scan (ABSCOR; Higashi, 1995)
T_{min} = 0.860, T_{max} = 1.000
6836 measured reflections
4249 independent reflections

4133 reflections with $I > 2\sigma(I)$
$R_{int} = 0.026$
$\theta_{max} = 27.5°$, $\theta_{min} = 2.4°$

$h = -11 \rightarrow 11$
$k = -12 \rightarrow 12$
$l = -14 \rightarrow 14$

Refinement

Refinement on F^2
Least-squares matrix: full
$R[F^2 > 2\sigma(F^2)] = 0.032$
$wR(F^2) = 0.080$
$S = 1.06$
4249 reflections
228 parameters
3 restraints

Primary atom site location: structure-invariant direct methods
Secondary atom site location: difference Fourier map
Hydrogen site location: mixed
$w = 1/[\sigma^2(F_o^2) + (0.037P)^2 + 0.6872P]$ where $P = (F_o^2 + 2F_c^2)/3$
$(\Delta/\sigma)_{max} = 0.001$
$\Delta\rho_{max} = 0.43$ e Å^{-3}
$\Delta\rho_{min} = -0.60$ e Å^{-3}

Special details

Geometry. All esds (except the esd in the dihedral angle between two l.s. planes) are estimated using the full covariance matrix. The cell esds are taken into account individually in the estimation of esds in distances, angles and torsion angles; correlations between esds in cell parameters are only used when they are defined by crystal symmetry. An approximate (isotropic) treatment of cell esds is used for estimating esds involving l.s. planes.

Fractional atomic coordinates and isotropic or equivalent isotropic displacement parameters (Å²)

	x	*y*	*z*	U_{iso}*/U_{eq}
Zn	0.76357 (3)	0.49975 (2)	0.25271 (2)	0.01863 (8)
S1	0.97385 (5)	0.65936 (5)	0.26357 (4)	0.01674 (11)
S2	0.69910 (6)	0.58080 (5)	0.03011 (5)	0.01835 (11)
S3	0.64889 (6)	0.27205 (5)	0.14638 (4)	0.01739 (11)
S4	0.90377 (6)	0.34805 (5)	0.38990 (4)	0.01782 (11)
O1	0.74043 (18)	0.85049 (17)	−0.09808 (15)	0.0260 (3)
H1O	0.695 (3)	0.783 (2)	−0.083 (3)	0.039*
O2	0.45844 (17)	0.01078 (16)	0.24736 (13)	0.0218 (3)
H2O	0.413 (3)	0.051 (3)	0.193 (2)	0.033*
O3	0.67339 (19)	0.91603 (16)	0.57620 (15)	0.0285 (3)
H3O	0.624 (3)	0.945 (3)	0.627 (2)	0.043*
N1	0.98304 (19)	0.70602 (17)	0.04700 (15)	0.0176 (3)
N2	0.78664 (19)	0.08741 (16)	0.26777 (15)	0.0161 (3)
N3	0.62518 (19)	0.59446 (17)	0.35049 (15)	0.0169 (3)
C1	0.8924 (2)	0.65371 (18)	0.10539 (18)	0.0149 (3)
C2	0.9350 (2)	0.6846 (2)	−0.09003 (18)	0.0191 (4)
H2A	0.8502	0.6046	−0.1285	0.023*
H2B	1.0271	0.6612	−0.1190	0.023*
C3	0.8749 (2)	0.8097 (2)	−0.1355 (2)	0.0221 (4)
H3A	0.9619	0.8882	−0.1017	0.027*
H3B	0.8450	0.7881	−0.2282	0.027*
C4	1.1446 (2)	0.7770 (2)	0.1154 (2)	0.0252 (4)
H4A	1.1454	0.8372	0.1951	0.038*
H4B	1.1789	0.8330	0.0647	0.038*
H4C	1.2175	0.7081	0.1321	0.038*

C5	0.7800 (2)	0.22057 (19)	0.26907 (17)	0.0143 (3)
C6	0.6826 (2)	−0.02451 (19)	0.16625 (18)	0.0181 (4)
H6A	0.7468	−0.0971	0.1421	0.022*
H6B	0.6353	0.0126	0.0920	0.022*
C7	0.5502 (2)	−0.0887 (2)	0.20439 (18)	0.0193 (4)
H7A	0.4796	−0.1595	0.1316	0.023*
H7B	0.5972	−0.1359	0.2718	0.023*
C8	0.8976 (2)	0.0451 (2)	0.3718 (2)	0.0232 (4)
H8A	1.0069	0.0797	0.3796	0.035*
H8B	0.8852	−0.0562	0.3554	0.035*
H8C	0.8751	0.0837	0.4499	0.035*
C9	0.6861 (2)	0.7161 (2)	0.43240 (18)	0.0175 (4)
H9	0.7921	0.7530	0.4436	0.021*
C10	0.6007 (2)	0.7911 (2)	0.50204 (18)	0.0194 (4)
C11	0.4471 (2)	0.7342 (2)	0.48828 (19)	0.0226 (4)
H11	0.3855	0.7818	0.5347	0.027*
C12	0.3863 (2)	0.6063 (2)	0.4053 (2)	0.0249 (4)
H12	0.2826	0.5646	0.3953	0.030*
C13	0.4768 (2)	0.5400 (2)	0.33723 (19)	0.0221 (4)
H13	0.4331	0.4534	0.2794	0.027*

Atomic displacement parameters (Å²)

	U^{11}	U^{22}	U^{33}	U^{12}	U^{13}	U^{23}
Zn	0.02010 (13)	0.01232 (12)	0.02810 (14)	0.00449 (9)	0.01447 (10)	0.00421 (9)
S1	0.0155 (2)	0.0171 (2)	0.0178 (2)	0.00248 (17)	0.00462 (17)	0.00523 (17)
S2	0.0154 (2)	0.0194 (2)	0.0201 (2)	0.00046 (17)	0.00437 (18)	0.00651 (18)
S3	0.0217 (2)	0.0157 (2)	0.0149 (2)	0.00533 (17)	0.00362 (18)	0.00587 (17)
S4	0.0180 (2)	0.0143 (2)	0.0184 (2)	0.00276 (16)	0.00247 (18)	0.00227 (17)
O1	0.0257 (8)	0.0311 (8)	0.0317 (8)	0.0137 (6)	0.0166 (7)	0.0160 (7)
O2	0.0232 (7)	0.0268 (8)	0.0184 (7)	0.0090 (6)	0.0094 (6)	0.0064 (6)
O3	0.0326 (8)	0.0227 (8)	0.0321 (8)	0.0011 (6)	0.0208 (7)	−0.0037 (6)
N1	0.0157 (7)	0.0191 (8)	0.0198 (8)	0.0025 (6)	0.0077 (6)	0.0058 (6)
N2	0.0165 (7)	0.0140 (7)	0.0165 (7)	0.0040 (6)	0.0024 (6)	0.0043 (6)
N3	0.0157 (7)	0.0179 (8)	0.0192 (7)	0.0071 (6)	0.0063 (6)	0.0062 (6)
C1	0.0160 (8)	0.0107 (8)	0.0193 (8)	0.0053 (6)	0.0071 (7)	0.0037 (7)
C2	0.0236 (10)	0.0199 (9)	0.0181 (9)	0.0071 (7)	0.0114 (8)	0.0058 (7)
C3	0.0250 (10)	0.0261 (10)	0.0232 (9)	0.0091 (8)	0.0140 (8)	0.0118 (8)
C4	0.0167 (9)	0.0301 (11)	0.0295 (11)	−0.0018 (8)	0.0078 (8)	0.0093 (9)
C5	0.0151 (8)	0.0149 (8)	0.0154 (8)	0.0046 (6)	0.0076 (7)	0.0038 (7)
C6	0.0217 (9)	0.0125 (8)	0.0177 (8)	0.0037 (7)	0.0053 (7)	−0.0004 (7)
C7	0.0215 (9)	0.0157 (9)	0.0195 (9)	0.0036 (7)	0.0047 (7)	0.0038 (7)
C8	0.0228 (10)	0.0181 (9)	0.0257 (10)	0.0065 (8)	−0.0005 (8)	0.0091 (8)
C9	0.0176 (9)	0.0180 (9)	0.0195 (9)	0.0059 (7)	0.0077 (7)	0.0066 (7)
C10	0.0221 (9)	0.0212 (10)	0.0173 (9)	0.0065 (8)	0.0080 (8)	0.0060 (7)
C11	0.0204 (9)	0.0311 (11)	0.0196 (9)	0.0094 (8)	0.0101 (8)	0.0058 (8)
C12	0.0139 (9)	0.0333 (12)	0.0256 (10)	0.0040 (8)	0.0061 (8)	0.0026 (9)
C13	0.0177 (9)	0.0264 (10)	0.0201 (9)	0.0037 (8)	0.0053 (8)	0.0016 (8)

Geometric parameters (Å, º)

Zn—N3	2.0375 (16)	C2—H2A	0.9900
Zn—S1	2.3319 (6)	C2—H2B	0.9900
Zn—S3	2.3437 (7)	C3—H3A	0.9900
Zn—S4	2.5275 (6)	C3—H3B	0.9900
Zn—S2	2.7514 (8)	C4—H4A	0.9800
S1—C1	1.733 (2)	C4—H4B	0.9800
S2—C1	1.7119 (19)	C4—H4C	0.9800
S3—C5	1.7364 (19)	C6—C7	1.518 (3)
S4—C5	1.7140 (19)	C6—H6A	0.9900
O1—C3	1.433 (2)	C6—H6B	0.9900
O1—H1O	0.833 (10)	C7—H7A	0.9900
O2—C7	1.418 (2)	C7—H7B	0.9900
O2—H2O	0.833 (10)	C8—H8A	0.9800
O3—C10	1.350 (2)	C8—H8B	0.9800
O3—H3O	0.834 (10)	C8—H8C	0.9800
N1—C1	1.333 (2)	C9—C10	1.393 (3)
N1—C4	1.468 (2)	C9—H9	0.9500
N1—C2	1.468 (2)	C10—C11	1.394 (3)
N2—C5	1.328 (2)	C11—C12	1.387 (3)
N2—C8	1.464 (2)	C11—H11	0.9500
N2—C6	1.466 (2)	C12—C13	1.379 (3)
N3—C9	1.337 (3)	C12—H12	0.9500
N3—C13	1.345 (3)	C13—H13	0.9500
C2—C3	1.516 (3)		
N3—Zn—S1	109.72 (5)	N1—C4—H4B	109.5
N3—Zn—S3	110.80 (5)	H4A—C4—H4B	109.5
S1—Zn—S3	139.04 (2)	N1—C4—H4C	109.5
N3—Zn—S4	103.07 (5)	H4A—C4—H4C	109.5
S1—Zn—S4	102.00 (2)	H4B—C4—H4C	109.5
S3—Zn—S4	74.41 (2)	N2—C5—S4	121.34 (14)
N3—Zn—S2	107.89 (5)	N2—C5—S3	121.19 (14)
S1—Zn—S2	70.825 (18)	S4—C5—S3	117.46 (11)
S3—Zn—S2	91.20 (2)	N2—C6—C7	112.02 (16)
S4—Zn—S2	148.839 (18)	N2—C6—H6A	109.2
C1—S1—Zn	90.54 (6)	C7—C6—H6A	109.2
C1—S2—Zn	77.85 (7)	N2—C6—H6B	109.2
C5—S3—Zn	86.67 (6)	C7—C6—H6B	109.2
C5—S4—Zn	81.43 (7)	H6A—C6—H6B	107.9
C3—O1—H1O	109 (2)	O2—C7—C6	112.50 (16)
C7—O2—H2O	113 (2)	O2—C7—H7A	109.1
C10—O3—H3O	110 (2)	C6—C7—H7A	109.1
C1—N1—C4	121.53 (17)	O2—C7—H7B	109.1
C1—N1—C2	122.52 (16)	C6—C7—H7B	109.1
C4—N1—C2	115.68 (16)	H7A—C7—H7B	107.8
C5—N2—C8	120.74 (16)	N2—C8—H8A	109.5

C5—N2—C6	122.91 (16)	N2—C8—H8B	109.5
C8—N2—C6	116.33 (15)	H8A—C8—H8B	109.5
C9—N3—C13	118.73 (17)	N2—C8—H8C	109.5
C9—N3—Zn	118.04 (13)	H8A—C8—H8C	109.5
C13—N3—Zn	123.22 (14)	H8B—C8—H8C	109.5
N1—C1—S2	122.54 (15)	N3—C9—C10	122.79 (18)
N1—C1—S1	118.66 (14)	N3—C9—H9	118.6
S2—C1—S1	118.79 (11)	C10—C9—H9	118.6
N1—C2—C3	113.44 (16)	O3—C10—C9	116.64 (18)
N1—C2—H2A	108.9	O3—C10—C11	125.07 (18)
C3—C2—H2A	108.9	C9—C10—C11	118.27 (19)
N1—C2—H2B	108.9	C12—C11—C10	118.52 (19)
C3—C2—H2B	108.9	C12—C11—H11	120.7
H2A—C2—H2B	107.7	C10—C11—H11	120.7
O1—C3—C2	112.64 (16)	C13—C12—C11	119.77 (19)
O1—C3—H3A	109.1	C13—C12—H12	120.1
C2—C3—H3A	109.1	C11—C12—H12	120.1
O1—C3—H3B	109.1	N3—C13—C12	121.87 (19)
C2—C3—H3B	109.1	N3—C13—H13	119.1
H3A—C3—H3B	107.8	C12—C13—H13	119.1
N1—C4—H4A	109.5		

C4—N1—C1—S2	175.51 (15)	Zn—S4—C5—S3	−1.66 (9)
C2—N1—C1—S2	−10.8 (2)	Zn—S3—C5—N2	−176.68 (15)
C4—N1—C1—S1	−4.7 (2)	Zn—S3—C5—S4	1.77 (10)
C2—N1—C1—S1	169.02 (14)	C5—N2—C6—C7	−103.9 (2)
Zn—S2—C1—N1	167.26 (16)	C8—N2—C6—C7	74.4 (2)
Zn—S2—C1—S1	−12.55 (9)	N2—C6—C7—O2	55.4 (2)
Zn—S1—C1—N1	−165.30 (14)	C13—N3—C9—C10	−2.0 (3)
Zn—S1—C1—S2	14.52 (10)	Zn—N3—C9—C10	178.55 (14)
C1—N1—C2—C3	102.8 (2)	N3—C9—C10—O3	−176.43 (17)
C4—N1—C2—C3	−83.2 (2)	N3—C9—C10—C11	2.1 (3)
N1—C2—C3—O1	−58.9 (2)	O3—C10—C11—C12	177.9 (2)
C8—N2—C5—S4	1.6 (3)	C9—C10—C11—C12	−0.5 (3)
C6—N2—C5—S4	179.87 (14)	C10—C11—C12—C13	−1.1 (3)
C8—N2—C5—S3	−179.97 (15)	C9—N3—C13—C12	0.2 (3)
C6—N2—C5—S3	−1.7 (3)	Zn—N3—C13—C12	179.67 (16)
Zn—S4—C5—N2	176.79 (16)	C11—C12—C13—N3	1.3 (3)

Hydrogen-bond geometry (Å, º)

Cg1 is the centroid of the (Zn,S3,S4,C5) chelate ring.

D—H···*A*	*D*—H	H···*A*	*D*···*A*	*D*—H···*A*
O1—H1*O*···S2	0.84 (2)	2.61 (2)	3.371 (2)	152 (3)
O2—H2*O*···O1^{i}	0.83 (3)	1.94 (3)	2.734 (2)	161 (3)

O3—H3*O*···O2^{ii}	0.84 (3)	1.79 (2)	2.619 (2)	170 (3)
C2—H2*B*···*Cg*1^{iii}	0.99	2.76	3.689 (2)	156

Symmetry codes: (i) −*x*+1, −*y*+1, −*z*; (ii) −*x*+1, −*y*+1, −*z*+1; (iii) −*x*+2, −*y*+1, −*z*.